Habitat disturbance interacts with *Bd* infection to shape the skin bacterial communities of an Amazonian frog

Lia Schlippe Justicia[1], Susana Ferreira[2], Franz Hoelzl[1, 3], Carolin Dittrich[1,4,5], Martin Mayer[6,7], Bibiana Rojas[1,5]

[1]Department of Interdisciplinary Life Sciences, Konrad Lorenz Institute of Ethology, University of Veterinary Medicine Vienna, Savoyenstraße 1, 1160 Vienna, Austria

[2]Department of Interdisciplinary Life Sciences, Research Institute of Wildlife Ecology, University of Veterinary Medicine Vienna, Savoyenstraße 1, 1160 Vienna, Austria

[3]Carinthia University of Applied Sciences, Europastraße 4, 9524 Villach, Austria

[4]Institute of Hydrobiology, Technische Universität Dresden, Zellescher Weg 40, 01217 Dresden, Germany

[5]University of Jyväskylä, Department of Biology and Environmental Science, P.O. Box 35, 40014, Jyväskylä, Finland

[6]Department of Forestry and Wildlife Management, University of Inland Norway, Anne Evenstads Vei 80, 2480 Koppang, Norway

[7]Department of Ecoscience, Aarhus University, Nordre Ringgade 1, 8000 Aarhus, Denmark

Abstract

Amphibians are the most threatened vertebrate class globally, with habitat alteration and the fungal pathogen *Batrachochytrium dendrobatidis* (*Bd*) representing two major and often co-occurring drivers of decline. However, how these stressors interact to shape host-microbiome-pathogen dynamics remains poorly understood. Here, we investigated whether variation in anthropogenic habitat disturbance, quantified using the Human Footprint Index (HFI), influences *Bd* infection patterns (prevalence and intensity) and skin bacterial community structure in six populations of the Neotropical poison frog *Dendrobates tinctorius*. We characterized alpha and beta diversity of both the overall skin bacterial community and the subset of putative *Bd*-inhibitory taxa. *Bd* infection probability increased with increasing HFI and with frog spatial proximity. While HFI alone had limited direct effects on skin microbiome composition, its interaction with *Bd* load was associated with reduced bacterial alpha diversity and increased community dispersion. Similarly, within the *Bd*-inhibitory bacterial subset, relative abundance was higher in frogs with both high *Bd* loads and in disturbed sites. Together, our findings suggest that anthropogenic disturbance may not directly restructure amphibian skin microbiomes, but instead intensifies pathogen-associated microbial changes, highlighting the importance of considering interacting global change stressors in amphibian disease ecology.

Keywords: Anthropogenic disturbance, *Dendrobates tinctorius*, disease ecology, poison frogs, skin microbiome.

1. Introduction

The symbiotic relationships between animals (as hosts) and the microbial communities that reside on and in their bodies have an enormous impact on their overall fitness (Rosenberg & Zilber-Rosenberg, 2018). This is due to the important function of microbiota in multiple processes including host development (McFall-Ngai et al., 2013), digestion (Gomaa, 2020), reproduction (Punzón-Jiménez & Labarta, 2021; Y. Wang & Xie, 2022), and immune system function (McFall-Ngai et al., 2013). In particular, the microbial communities associated with the skin (i.e. skin microbiome) have been shown to play a critical role in protecting multiple species from diseases by directly inhibiting pathogens (Flowers & Grice, 2020). This inhibition is achieved thanks to the capability of some skin microbes to produce antimicrobial peptides and other molecules that can kill or alter the virulence of pathogens (Woodhams et al., 2018; Nakatsuji et al., 2021). At the same time, however, pathogen exposure and/or infection can alter the structure and composition of the skin microbiome (Jani & Briggs, 2014; Bates et al., 2022), potentially increasing further susceptibility to recurrent or novel infections.

These already complex host-microbiome-pathogen interactions can be further influenced by multiple host-specific, environmental and anthropogenic factors. For example, the skin microbiome can be strongly shaped by biogeographic conditions such as elevation, temperature and precipitation (Ruthsatz et al., 2020; Li et al., 2023), as well as by anthropogenic stressors like habitat fragmentation (Becker et al., 2017) and pollutants (Preuss et al., 2020; Mousavi et al., 2022). Therefore, given the alarming rates of habitat loss and fragmentation in many parts of the world (Haddad et al., 2015; Sage, 2020; Socolar et al., 2025), studies looking at the effects of habitat disturbance on the interactions between commensal and pathogenic microorganisms on the host microbiome are highly important to understand the vulnerability of animal populations to emerging pathogens and diseases.

Amphibians have experienced global population declines since the 1980s due to both habitat disturbances (Beebee & Griffiths, 2005; Womack et al., 2022; Luedtke et al., 2023) and the pathogenic fungus *Batrachochytrium dendrobatidis* (hereafter *Bd*), which causes the infectious disease chytridiomycosis (Berger et al., 1998; Scheele et al., 2019). *Bd* infects the keratinized epidermal cells of amphibians, often disrupting key physiological functions such as osmoregulation (Voyles et al., 2009). Although this disease can be lethal in many cases, there is a great variation in susceptibility among species and populations (Woodhams et al., 2007; Savage & Zamudio, 2011), which has been partly explained by differences in the skin microbiome (Woodhams et al., 2014; Bates et al., 2022). For instance, certain bacterial species can produce antifungal metabolites which inhibit *Bd* growth (Harris et al., 2006; Woodhams et al., 2018), while fungi have also been associated with host defence against pathogens (Kearns et al., 2017). Thus, if anthropogenic habitat disturbance alters the amphibians' skin microbiome, it could also increase their susceptibility to infection (Piovia-Scott et al., 2017; Ellison et al., 2019). In addition, *Bd* prevalence itself might be directly or indirectly favoured by anthropogenic activities (Bacigalupe et al., 2017; Siddons et al., 2020; Alvarado-Rybak et al., 2021; de Andrade Serrano et al., 2022), although the relationship between disturbance and infection dynamics is complex and context-dependent. Pristine forests might, for instance, offer favourable environmental conditions for the pathogen, enhancing its impacts (Becker & Zamudio, 2011).

The dyeing poison frog, *Dendrobates tinctorius,* is an emblematic species endemic to the Guiana Shield, where it is widespread (Rojas & Pašukonis, 2019) despite its patchy distribution associated with upland forest habitats (Noonan & Gaucher, 2006). Throughout their geographic range, these frogs are subject to different anthropogenic pressures including urbanization, agriculture, logging and mining activities and, since 2009, *Bd* has been reported to occur in some populations (Courtois et al., 2012, 2015). While there is currently no evidence of *Bd*-associated population declines, long-term demographic data for this species is extremely limited. Furthermore, the way anthropogenic habitat disturbance and the skin

98 microbiome interact in affecting patterns of *Bd* infection in this and other species in the wild is
99 still poorly understood, with only a few studies beginning to address these interactions (e.g.,
100 Jiménez et al., 2020; Neely et al., 2022).
101
102 Here, we investigated whether anthropogenic habitat disturbance is associated with *Bd*
103 infection dynamics and variations in the skin bacterial communities of *D. tinctorius*, and how
104 these three factors interact. We also examined whether skin microbiome alterations are
105 accompanied by shifts in putative *Bd*-inhibitory taxa, with potential implications for host
106 susceptibility. To do so, we surveyed the skin bacterial communities (amplicon sequencing
107 variants) and *Bd* infection (status and intensity) of *D. tinctorius* across six sites under different
108 levels of disturbance, and quantified differences for the whole skin bacterial communities, as
109 well as for the putative *Bd*-inhibitory subset. We predicted that:
110 (1) Prevalence and intensity of *Bd* infection would be higher in more disturbed sites, via several
111 potential non-exclusive mechanisms (e.g., disturbance may alter spatial distribution, leading
112 to higher local densities or greater aggregations of frogs due to fewer available habitat
113 patches, increasing transmission rates).
114 (2) Individuals would exhibit differences in the alpha and beta diversity of their skin bacterial
115 communities in relation to *Bd* infection, and conditional on human disturbance. In accordance
116 with the Anna Karenina Principle, which predicts that stressed hosts diverge from a common
117 healthy microbial state in different ways (Zaneveld et al., 2017), we would expect *Bd*-free frogs
118 to have higher alpha diversity but more similar community composition among individuals,
119 whereas infected frogs should exhibit lower alpha diversity but greater among-individual
120 dispersion in community composition, indicative of a dysbiotic microbial state. Moreover, we
121 would expect these patterns to be mediated by habitat disturbance, with infection-related
122 effects on the skin bacterial communities being comparatively less pronounced in pristine than
123 in human-impacted habitats.

(3) Infected individuals would show relatively lower diversity and abundance of putative *Bd*-inhibitory bacteria. We expect the same pattern to be found in individuals from disturbed sites, where we predict *Bd* prevalence to be higher.

2. Materials and Methods

2.1 Field sampling

From January to March 2023, we conducted field surveys in six study sites across French Guiana (ranging from 17 to 228 m above sea level), with an average survey effort of approximately 41 hours per site (range: 35 – 51 h). Sites were selected to represent a gradient of habitat disturbance: two study sites (Nouragues and Kaw) were located in pristine forests within protected natural reserves, two sites were in areas moderately disturbed by forestry (Mataroni) or agriculture (Cacao), and two sites were in highly fragmented habitats surrounded by urbanization (Petit Matoury and Mont Fortuné). To assign a quantitative measure of human pressure to each site, we used the Human Footprint Index (HFI) at 1000 m resolution, which scores human influence based on eight variables integrating accessibility, land use, population density, and infrastructure (Mu et al., 2022) (Fig. 1).

Along transects at each site, we conducted visual surveys and recorded the GPS coordinates of every *D. tinctorius* individual detected using a handheld GPS (Garmin GPSMAP 64). Up to 50 frogs per site were captured by hand, using a new pair of nitrile gloves for each individual to prevent cross-contamination. Skin swabs were collected by gently rotating a sterile nylon-flocked swab (4N6FLOQSwabs, ThermoFisher Scientific™) five times over the dorsum, ventrum, thighs, each side of the body, and feet. Swabs were immediately stored individually in DNA/RNA-shield (Zymo Research Corp, Irvine, CA), which halts microbial activity (including proliferation) and preserves DNA integrity at room temperature for at least 24 months.

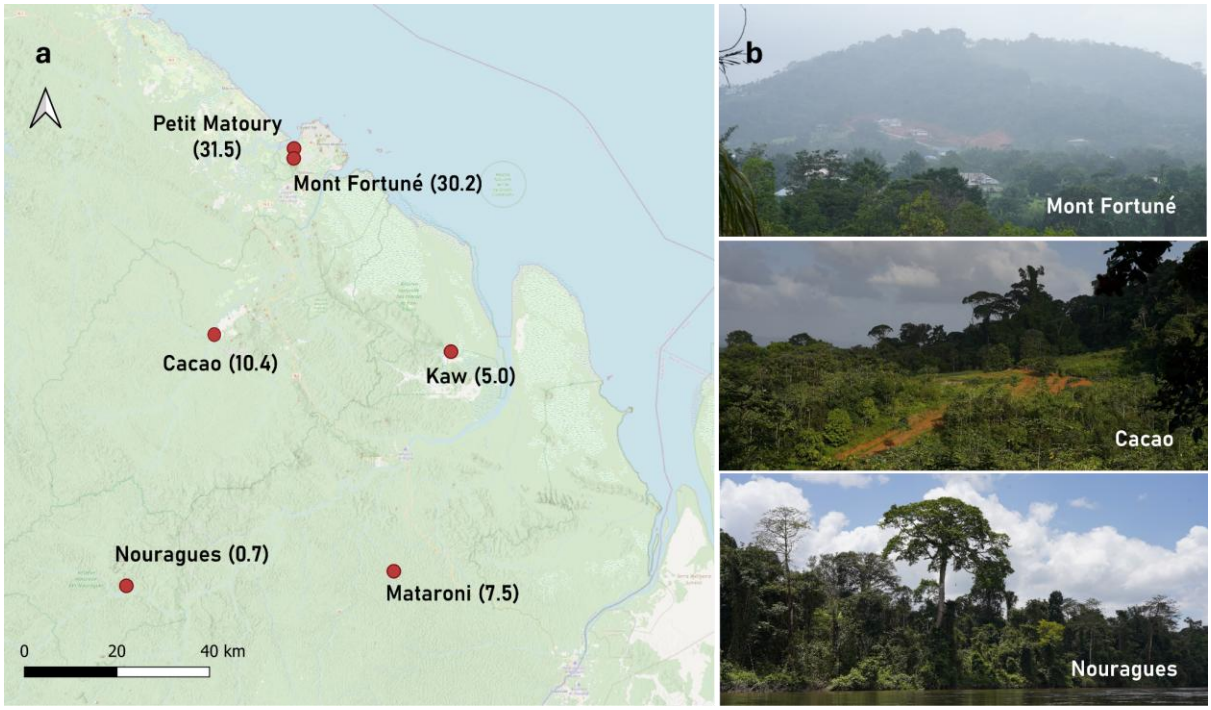

Fig. 1. (a) Map showing the six study populations (red dots) with the mean Human Footprint Index value for each location shown in brackets. (b) Photographs from three of the study sites, arranged from higher HFI (top) to more pristine conditions (bottom). Photos: © Martin Mayer

After swabbed, frogs were weighed to the nearest 0.01 g, sexed based on fingertip width relative to body size (Rojas & Endler, 2013), and photographed on millimetre paper for individual identification and snout-vent length (SVL) measurement. All frogs were released at the point of capture immediately after sampling. Field equipment was disinfected with ethanol between sites and between each frog measured to minimize the risk of *Bd* spread.

In addition, at each study site we collected three environmental swab samples of different terrestrial substrates potentially used by *D. tinctorius* (e.g. leaf litter, phytotelmata, soil). We also obtained 18 skin swabs from first-generation captive-bred *D. tinctorius* individuals originating from five different populations and reared under standardized conditions in a research colony at premises of the Laboratoire Ecologie, Evolution, Interactions des Systèmes Amazoniens (LEEISA) in Cayenne, French Guiana. Environmental samples were used to control for transient environmental bacteria (i.e. not associated with the frogs' skin

167 microbiome), whereas colony samples were collected to help disentangle whether potential
168 microbiome differences between populations were caused by environmental or genetic
169 effects. All samples were processed equally during storage, DNA extraction, amplification, and
170 sequencing.
171
172 *2.2 DNA extraction and sequencing*
173 We extracted bacterial community DNA from frog skin and environmental swabs using the
174 Quick-DNA Magbead Plus Kit (Zymo Research, Irvine, CA) following the manufacturer's
175 protocol for microbial samples. A blank sample (DNA/RNA-shield only) was included in each
176 round of extractions as a control against contamination of working solutions. The quantity of
177 DNA was measured using the Qubit 2.0 Fluorometer and the Qubit dsDNA HS Assay Kit
178 (Thermo-Fisher Scientific). DNA extracts were sent individually in 1.5 mL tubes for amplicon
179 library preparation and Next Generation Sequencing (NGS) to Novogene Europe laboratory
180 (Cambridge, UK). The V3-V4 hypervariable regions of the bacterial 16S rRNA gene were
181 amplified with bacterial primers 341F (5′-CCTAYGGGRBGCASCAG-3′) and 806R (5′-
182 GGACTACNNGGGTATCTAAT-3′) (465 bp fragment) (Yu et al., 2005). The sequencing was
183 done as pair-end reads of 250 bp on an Illumina NovaSeq 6000 by Novogene Europe
184 laboratory UK.
185
186 *2.3 ddPCR*
187 Quantification of *Bd* and *D. tinctorius* DNA from skin swabs followed the protocol described in
188 Schlippe-Justicia et al. (2026). Briefly, DNA extracts were processed and read on a Bio-Rad
189 QX200 Droplet Digital PCR (ddPCR) system under standard conditions including species-
190 specific primers and probes for *Bd* and *D. tinctorius* (see Schlippe-Justicia et al., 2026). Each
191 run included negative (non template) and positive (*Bd* and *D. tinctorius* DNA) controls, and
192 samples were considered *Bd*-positive only if at least three positive droplets were detected
193 across duplicate runs (Taugbøl et al., 2021).
194

195 *2.4 Bioinformatics*

196 All analyses were performed using R v 4.4.2 (R Core Team, 2024). Demultiplexed and
197 adapter-trimmed sequence reads were processed using the package *dada2* v. 1.32.0
198 (Callahan et al., 2016). Reads were quality-filtered (truncQ = 2, maxN = 0, maxEE = c(2,2),
199 PhiX removed), denoised, merged (default, minimum of 12 bp overlap), sorted by abundance
200 and chimaera-removed (method = consensus), following the DADA2 pipeline
201 (https://benjjneb.github.io/dada2/tutorial.html).

202

203 Amplicon sequence variants (ASVs) were taxonomically assigned using the RDS classifier (Q.
204 Wang et al., 2007) implemented in *dada2*, using the SILVA 138.1 SSU Ref NR 99 database
205 (Quast et al., 2013; McLaren & Callahan, 2021). The resulting ASV table, taxonomy table, and
206 sample metadata were then merged into a phyloseq object using the *phyloseq* (McMurdie &
207 Holmes, 2013) and *Biostrings* (Pages et al. 2025) packages and used for all downstream
208 analyses.

209

210 Potential contaminant ASVs were identified with *decontam* v. 1.21.0 (Davis et al., 2018) using
211 the “prevalence” method (default threshold of 0.1), resulting in the removal of 429 ASVs. Low-
212 prevalence taxa present in fewer than 3% of samples (less than 9 samples) were removed
213 using the *microbiome* package (Lathi et al. 2020). Following decontamination, only bacterial
214 ASVs were retained by removing taxa assigned to non-bacterial kingdoms, as well as
215 chloroplast and mitochondrial sequences, resulting in 6738 ASVs. Sample library sizes ranged
216 from 9,229 to 43,337 reads per sample (median = 24,605). No rarefaction was applied;
217 sequencing depth was accounted for statistically in downstream analysis.

218

219 *2.5 Bd-inhibitory ASVs*

220 To identify putatively *Bd*-inhibitory bacterial taxa within our wild frogs’ skin microbiome, we
221 used the database of amphibian skin bacterial isolates compiled by Woodhams et al., (2015)
222 (https://github.com/AmphiBac/AmphiBac-Database), which includes 16S rRNA sequences

from cultured bacterial taxa with known *Bd* inhibiting properties. Because our microbiome sequencing targeted the V3–V4 region of the 16S rRNA gene, we first standardized the Woodhams reference sequences to the same region. Using exact primer searches (including reverse complements), we extracted the V3-V4 amplicon from each isolate sequence, retaining only isolates in which both primer positions could be unambiguously located. This trimming avoids inflated similarity values derived from matches outside the sequenced region. A total of 906 Woodhams isolates had a successful amplicon match and were saved as a curated reference FASTA.

ASVs sequences extracted from the phyloseq object were then searched against this curated database using BLASTn (tabular output, outfmt 6). We applied a ≥ 97% identity-threshold (corresponding to classical species-level similarity thresholds; Stackebrandt & Goebel, 1994). BLAST hits were retained and ASVs defined as *Bd*-inhibitory if the percent identity exceeded this threshold. ASVs with no BLAST hit were conservatively classified as non-inhibitory. *Bd*-inhibitory status was then merged into the taxonomy table of the phyloseq object, generating the dataset used for the subsequent diversity and abundance analyses. Importantly, in-vitro *Bd* inhibition assays do not necessarily mirror how bacteria function in natural conditions, and require further experimental validation to confirm true anti-pathogen activity (Woodhams et al. 2015).

2.6 Spatial data, human footprint index, and body condition

To obtain scores of anthropogenic disturbance, we overlaid the frog GPS coordinates on the HFI raster using QGIS 3.34 (Geographic Information System), and extracted the corresponding HFI value for each frog location. Relative population densities were estimated by calculating the number of individuals observed per km transect for each day, and then averaging the daily estimates for each population, as reported in a previous study (Mayer et al., 2025). To quantify spatial aggregation of frogs within each site, we used their spatial coordinates to calculate the nearest neighbour distance (NND), defined as the Euclidean

distance to the closest conspecific, using the function *nn2* from package *RANN* v. 2.6.2 (Jefferis et al., 2025). NND was measured across all individuals within each site, pooling locations across days under the assumption of limited frog movement during the short sampling periods within populations (mean survey effort = 41 h per site), which were spread over 4 – 32 calendar days (mean = 13.3 days), depending on site logistics. In addition, we estimated the local density by counting the number of individuals located within a 15 m radius around each frog, a distance that encompasses the reported short-term home range of the species (~ 200 m²; Pašukonis et al., 2022). Finally, substantial phenotypical differences in body size among populations resulted in differences in body condition estimates, making among-population comparisons unreliable. Thus, we calculated the scaled mass index (SMI) separately for each population following Peig & Green (2009, 2010), reflecting within-population conditions only.

2.7 Statistical analyses

2.7.1 Infection patterns

To test whether anthropogenic disturbance influences the probability of *Bd* infection or its intensity, we modelled *Bd* infection status (*Bd*+, *Bd*-) and *Bd* load (log-transformed; including infected individuals only) as a function of the HFI and individual-level predictors potentially associated with infection risk. These included sex, SMI, SVL, distance to the nearest conspecific (NND), local density, elevation, and the interactions between sex and SVL (to account for sexual size dimorphism), and SMI and HFI (to explore potential synergetic effects).

We initially fitted mixed-effects models using study site as a random intercept to account for potential non-independence of individuals within populations. However, HFI values were nearly identical for all individuals within sites, leading to singular fit and indicating that the random effect explained negligible variance. Consequently, we used a generalized linear model (GLM) with a binomial distribution and logit link for *Bd* probability, and a standard linear model for *Bd* load.

To explore potential mechanisms by which HFI could influence infection probability, we tested specific hypotheses using separate models. First, we examined whether frogs were more spatially aggregated in disturbed sites by modelling NND (log-transformed) as a function of HFI, using a linear model with Gaussian distribution, while accounting for potential sex differences in space use and relative population density. Similarly, we modelled local density (number of neighbours) using a negative binomial generalized linear model with the same predictors as above. Second, we tested whether population-level density was correlated with the mean HFI using a Spearman rank correlation test.

2.7.2 Microbiome diversity

To test whether habitat disturbance and *Bd* infection were associated with the alpha diversity of the overall skin bacterial community or the putative *Bd*-inhibitory taxa, we calculated two diversity indices for each individual: Chao1 richness (Chao, 1984) and Shannon diversity index (Shannon, 1948), using the phyloseq object from our bioinformatic pipeline. For each alpha diversity metric (response variable), we fitted a linear model including HFI, *Bd* infection (infection status or log-transformed *Bd* load, in separate models), their interaction, sex (juvenile, male, or female), and body condition. To account for potential biases due to differences in sequencing effort between samples, we also included log-transformed sequence read depth as a covariate.

We quantified variation in the skin bacterial community among samples by calculating Bray-Curtis pairwise distances (β-diversity) based on ASV abundance tables (Bray & Curtis, 1957). Dissimilarity distances were computed using the “distance” function in the *vegan* package v. 2.6-4 (Oksanen et al. 2022) and then converted to similarity values (1 - Bray-Curtis distance) for interpretability. These analyses were conducted both for the overall bacterial community and for the subset of putative Bd-inhibitory taxa.

To test which factors explained differences in the skin bacterial composition among individuals (β-diversity), we modelled pairwise similarity distances (excluding self-comparisons) as a response variable, as previously described (Raulo et al., 2021; Ferreira et al., 2024; Soares et al., 2025). Predictor variables were expressed as pairwise distances between individuals. Host-related predictors included age class (same vs. different). Environmental predictors included spatial distance and differences in HFI. Infection-related predictors were differences in *Bd* load, and the interaction between *Bd* load differences and HFI differences. To assess potential sex effects, we performed an additional model including only adult individuals (N = 216), including the same predictor set.

Analyses were conducted using Bayesian generalized linear multilevel models fitted with the No-U-Turn Sampler (NUTS) Markov chain Monte Carlo algorithm (Hoffman et al. 2014) implemented in Stan, accessed through the *brms* package v. 2.19.0 (Bürkner et al. 2017). We used a multi-membership random-effects framework to model individual contributions within pairwise comparisons (e.g., Individual A, Individual B). All predictors were rescaled to a 0 - 1 range for standardized estimate comparison. We ran four Markov chains, each with 3,000 iterations (1,000 warm-up), using weakly informative priors. Convergence was confirmed through visual inspection, and predictor importance was determined by R-hat values (accepted if < 1.01) and 95% CI. As a robustness check, we repeated analyses using Jaccard distances (presence-absence). As results were consistent, we reported those based on Bray-Curtis distances.

Finally, to test whether overall microbiome variability increased with *Bd* infection intensity, HFI, or their interaction, we quantified multivariate dispersion. Using the previously computed Bray-Curtis dissimilarity matrices, we calculated each individual's distance to a global centroid using the "betadisper" function in *vegan*, assigning all samples to a single dummy group to obtain an individual-level measure of dispersion. These distances were then used as response variables in linear models including *Bd* load, HFI, and their interactive effect.

335 2.7.3 Model checks

336 Across all analyses, none of the predictors were highly correlated (Pearson correlation
337 coefficient < 0.4). All continuous predictors were scaled and centred to facilitate model
338 convergence and allow direct comparison of effect sizes. Model fit and assumptions were
339 validated through diagnostic checks for dispersion and deviation using the *DHARMa* package
340 v. 0.4.7 (Hartig, 2022). We considered parameters uninformative (i.e. statistically unclear) if
341 their 95% confidence or credible intervals (CI) included zero (Arnold, 2010). To account for
342 non-independence of observations within sites, we adjusted statistical inference by using
343 cluster-robust standard errors and confidence intervals. These were obtained using the
344 packages *sandwich* v. 3.1.1 (Zeileis et al., 2019) and *lmtest* v. 0.9.40 (Hothorn et al., 2015),
345 with site specified as the clustering unit. Data visualization was performed using the package
346 *ggplot2* v. 4.0.0 (Wickham, 2016), and all analyses were performed in R v. 4.4.2 (R Core
347 Team, 2024).

348

349 **3. Results**

350 *3.1 Effects of habitat disturbance on infection dynamics and host traits*

351 We encountered a total of 277 unique *D. tinctorius* and collected one skin swab from 239
352 individuals to determine their infection status (Table 1). Overall, *Bd* infection prevalence was
353 20.5%, with infected frogs detected in all study sites, including juvenile frogs. However,
354 probability of infection differed significantly between study sites, with *Bd* prevalence being the
355 highest in Mont Fortuné (45.9%) and lowest in Cacao (7.1%) (Table 1). *Bd* loads ranged from
356 0.2 to 2027 copies/µl (mean ± SD: 169.5 ± 407.7) (Table 1), but most infected frogs had
357 relatively low infection load (≤100 copies/µl), with only 11 individuals exceeding this threshold.

358

359

360 **Table 1.** Summary of the number of *Dendrobates tinctorius* sampled per frog class and population, the
361 proportion of frogs infected with *Batrachochytrium dendrobatidis* (prevalence), and the mean *Bd* load
362 with total range.

	Individuals swabbed	*Bd* prevalence (%)	Mean *Bd* load (range)
Frog class			
Juveniles	15	13	214.44 (41.25 – 387.64)
Females	135	24	153.79 (0.20 – 1451.67)
Males	89	17	197.12 (0.21 – 2027.10)
Study site			
Nouragues	50	14	108.03 (0.20 – 417.25)
Kaw	50	16	29.81 (0.21 – 167.67)
Mataroni	50	16	42.85 (0.31 – 243.57)
Cacao	14	7.1	1.14
Mont Fortuné	37	46	150.02 (0.26 – 1451.67)
Petit Matoury	38	21	552.23 (0.37 – 2027.10)

363

364 The probability of *Bd* infection increased with increasing HFI and with decreasing distance to
365 the closest frog (Table S1a; Fig. 2). None of the other variables were informative. In contrast,
366 *Bd* loads were not explained by HFI or frog spatial distribution, but were negatively associated
367 with frog body size (Table S1b).

368

369 When testing the potential mechanisms for the higher probability of *Bd* infection in disturbed
370 sites, we found no evidence that frog aggregation (measured both as nearest-neighbour
371 distance and local density) increased with disturbance level (Table S2a-b). Instead, patterns
372 of spatial clustering were primarily explained by relative population density, with frogs
373 occurring closer together in denser populations, and by sex class, with males exhibiting shorter
374 NND than females, and juveniles occurring in locally denser areas (Table S2a-b). Similarly,
375 HFI was not correlated with relative population density (Spearman's $\rho = -0.31$, $p = 0.56$).

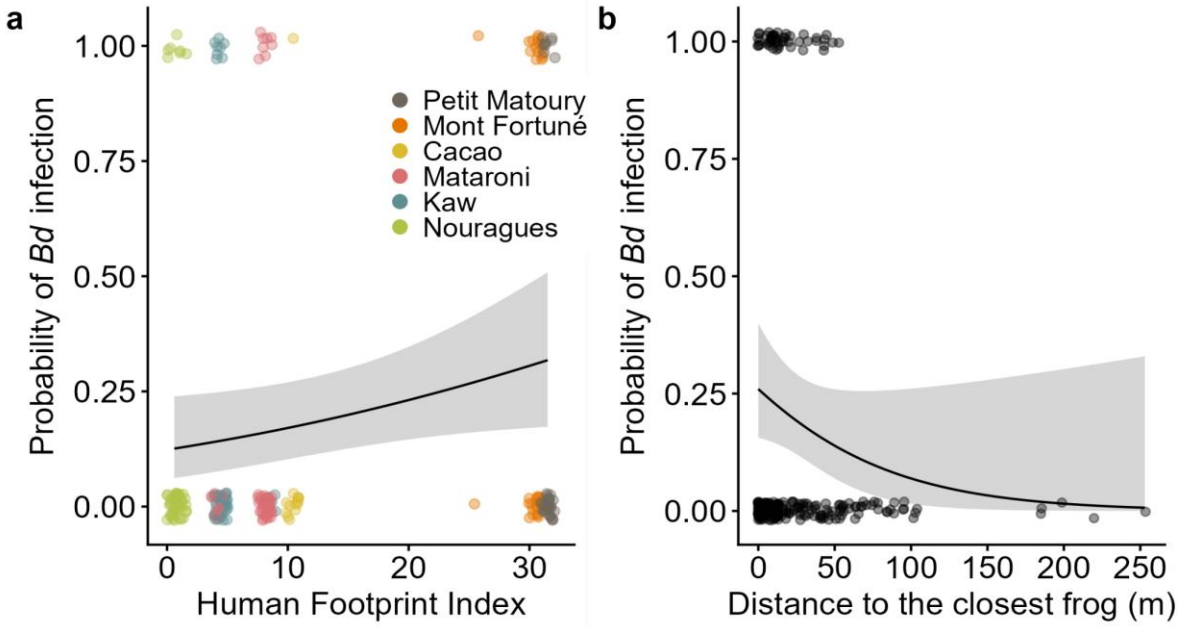

Fig. 2. Predicted effect of (a) HFI and (b) NND on the probability of *Bd* infection for all populations. Lines represent model predictions with 95% CI; raw data points are shown as dots (coloured by population in plot a).

3.2 Microbiome composition across sample types

We profiled the skin bacterial community of 230 wild and 18 colony-raised *D. tinctorius* individuals, along with 23 environmental samples (Fig 3a). Out of 230 wild *D. tinctorius*, 216 were adults (130 females and 86 males) and 14 were juveniles. The overall skin bacterial community of wild frogs was composed of 6663 ASVs belonging to 31 phyla, and 709 ASVs belonging to unknown phyla (Fig. 3b), while colony frogs harboured 2671 ASVs from 27 phyla, and 277 ASVs from unknown phyla. The environmental microbiome contained 4603 ASVs from 29 phyla and 480 ASVs from unknown phyla. Pairwise comparisons indicated that community composition differed significantly among the three sample types (PERMANOVA: all $p < 0.01$; $F = 6.98 - 11.69$; $R^2 = 0.03 - 0.15$). Wild frogs were dominated by Proteobacteria, Actinobacteriota, Acidobacteriota, and Bacteroidota, which together accounted for ~74.6% of total ASV abundance. Other consistently detected but less abundant phyla included Myxococcota, Verrucomicrobiota, Chloroflexi, and Firmicutes (Fig. 3b).

Across all wild frog samples, 474 ASVs (7.1% of total ASVs) matched bacteria taxa associated with *Bd* inhibitory functions (at ≥ 97% sequence similarity) and collectively accounted for ~10% of sequencing reads. On average, frogs had 52 anti-*Bd* ASVs (SD ± 19) on their skin. The ten most abundant *Bd*-inhibitory ASVs collectively accounted for 33.9% of all inhibitory bacterial reads. The most dominant genus was Variovorax (*Variovorax paradoxus*, family Comamonadaceae), comprising 12.5% of all inhibitory reads, followed by Marivivens (*Marivivens donghaensis*, Rhodobacteraceae) at 5.6%. Other predominant inhibitory taxa included *Pseudomonas aeruginosa* (Pseudomonadaceae), Candidatus Nostocoida (Isosphaeraceae), Chryseobacterium (Weeksellaceae), Stenotrophomonas (Xanthomonadaceae), members of the Allorhizobium–Neorhizobium–Pararhizobium–Rhizobium complex (Rhizobiaceae), and several unclassified bacterial lineages. These top inhibitory ASVs were detected at moderate to high prevalence across individuals (11 – 91%).

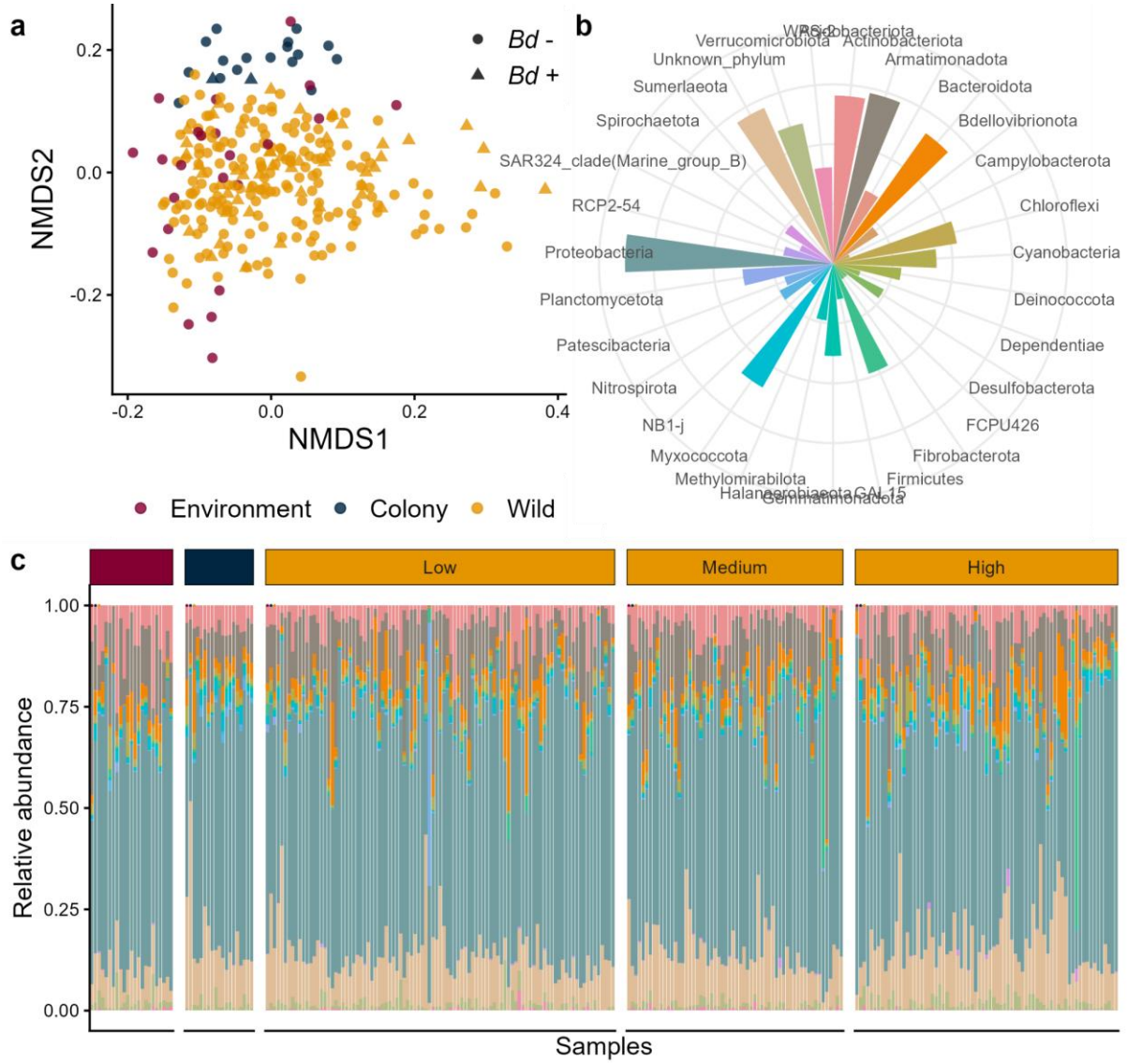

Fig. 3. (a) Non parametric multidimensional scaling (NMDS) of the overall bacterial composition for all samples (n = 271). Samples are coloured by source: skin of wild frogs (n = 230), colony frogs (n = 18) and environmental samples (n = 23). (b) The number of amplicon sequence variants (ASV) per phylum for skin of wild frogs. Colours represent the different phyla. (c) The relative abundance of each ASV (y-axis) for each sample (x-axis) for environmental samples, colony frogs and wild frogs, respectively. The wild frogs are grouped by sites with low (Nouragues, Kaw), intermediate (Cacao, Mataroni) and high (Petit Matoury, Mont Fortuné) human footprint index.

3.3 Skin microbiome association to Bd infection, HFI and frog traits

3.3.1 Alpha diversity

Chao1 richness ranged from 65 to 1073 and Shannon diversity from 1.35 to 6.33. Across populations, diversity was highest in Cacao (Chao1: 728 ± 143; Shannon: 5.53 ± 0.52), followed by Mont Fortuné (Chao1: 620 ± 191; Shannon: 5.08 ± 0.79), Nouragues (Chao1: 604 ± 234; Shannon: 4.94 ± 0.91), Mataroni (Chao1: 582 ± 212; Shannon: 4.61 ± 0.95) and Kaw (Chao1: 538 ± 222; Shannon: 4.64 ± 0.96), and was lowest in Petit Matoury (Chao1: 533 ± 235; Shannon: 4.57 ± 1.08).

Alpha diversity was not associated with *Bd*-infection status, HFI, or the interaction between the two (Table S3a). However, when analysing the subset of infected individuals, Shannon diversity decreased with increasing *Bd* load (trend only for Chao1; see Table S3b). Notably, the interaction between *Bd* load and HFI significantly affected Shannon diversity, with stronger negative associations at higher HFI values (Table S3b; Fig. 4a). Across both models, juvenile frogs consistently showed lower alpha diversity than adults and body condition was positively associated with diversity. Sequence depth also had a positive effect on Chao1 estimates in both models (Table S3a-b).

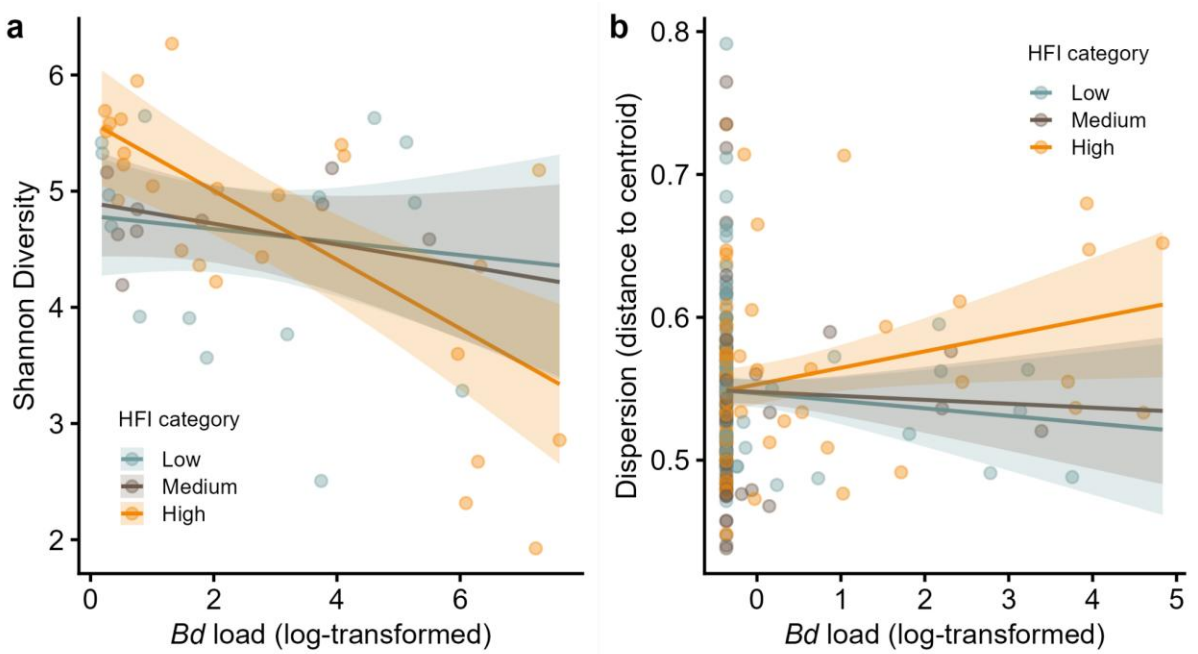

Fig. 4. (a) For infected individuals only, effect of the interaction between *Bd* load (log-transformed) and Human Footprint Index (HFI) on Shannon diversity, and (b) effect of the same interaction on the skin bacterial community dispersion, measured as the distance to the group centroid using Bray-Curtis distances. HFI was treated as a continuous variable in the models but grouped into three categories for visualization only (Low: HFI < 5; Medium: 5 – 19; High: > 19).

3.3.2 Beta diversity and dispersion

Infection load and spatial distance were the strongest predictors of variation in the skin bacterial composition (Table S4; Fig. 5). Higher differences in *Bd* load between individuals were associated with marked declines in microbiome similarity, showing that infection intensity was a key driver of community turnover. Similarly, greater geographic distance between frogs lead to lower bacterial similarity. HFI exhibited a weak but positive association with microbiome similarity, suggesting that frogs from habitats that differ more strongly in HFI tended to exhibit more similar skin bacterial communities. The interaction between HFI and *Bd* load did not show an effect, suggesting that the influence of infection intensity on microbiome dissimilarity was independent of habitat disturbance (Table S4; Fig. 5).

Age class showed a positive effect, with frogs within the same age category (adults vs. juveniles) harbouring more similar skin bacterial assemblages. These patterns remained consistent when restricting to adult frogs only (Table S4; Fig. 5).

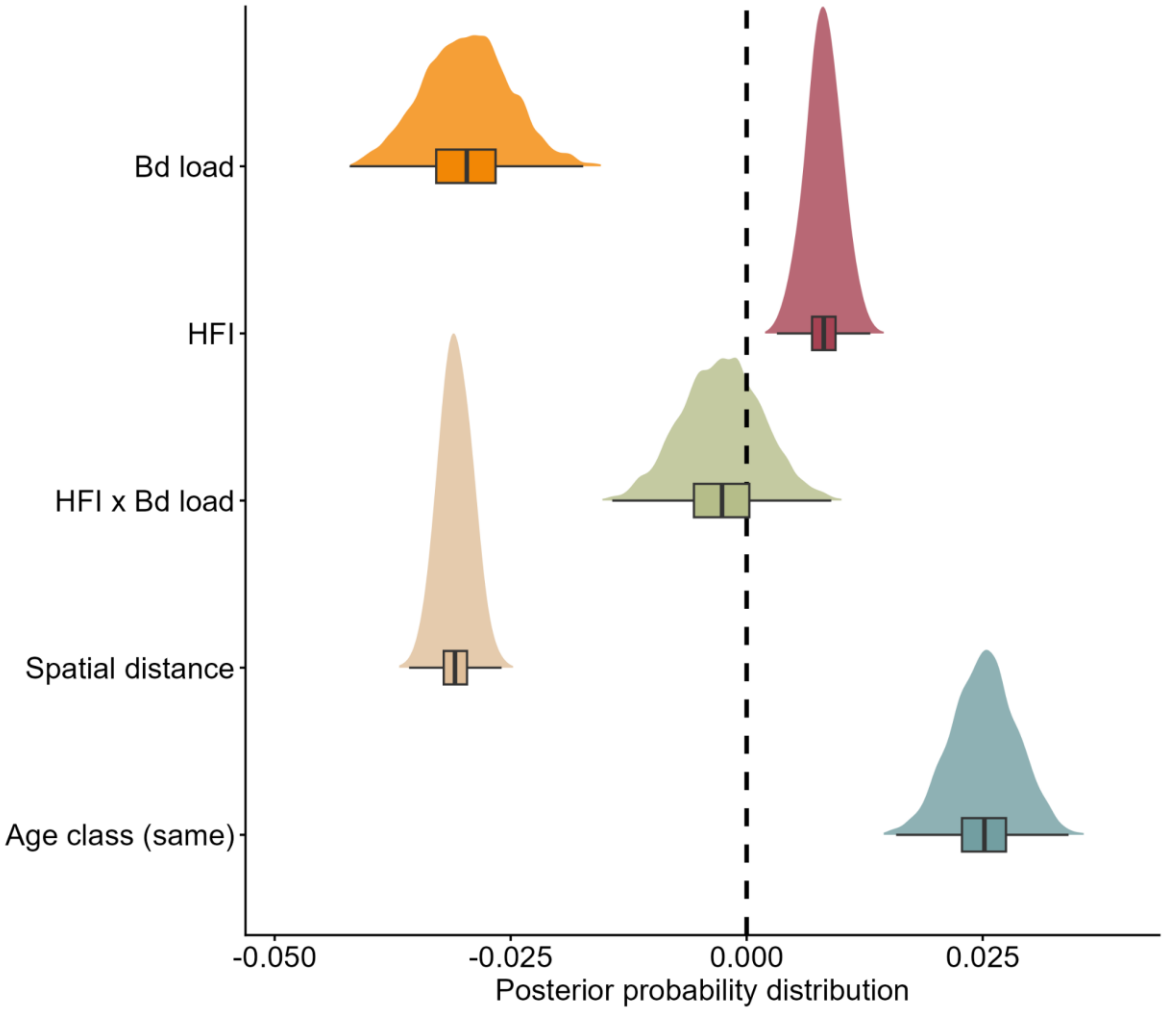

Fig. 5. Compositional differences (ß-diversity) of skin bacterial communities across 230 wild *D. tinctorius* individuals, based on 6663 ASVs. Pairwise Bray-Curtis similarity (response variable) were analysed using a Bayesian multilevel model. Predictors included differences in infection load, HFI, an interaction between the two, spatial distance, and age class (same vs. different). Individual ID of each pairwise comparison was included as a multi-membership random effect. Shown are the densities and boxplots of the posterior effect sizes.

Neither *Bd* load nor HFI alone were associated with changes in microbial dispersion (Table S5). However, their interaction had a significant positive effect, indicating that microbiome variability increased with *Bd* load only under high levels of habitat disturbance (Table S5; Fig 4b).

3.3.3 Putative anti-*Bd* ASVs

The relative abundance of inhibitory ASVs did not differ between infected and uninfected frogs (Table S6a). Among infected individuals, relative abundance increased with *Bd* load at sites with higher HFI, indicating a positive interaction between *Bd* load and habitat disturbance (Table S6b; Fig. S1b). Body condition was also positively associated with inhibitory ASV abundance, whereas sex did not explain variation in either model (Table S6a-b). Alpha diversity of *Bd*-inhibitory ASVs was not associated with frog body condition, *Bd* infection status (or *Bd* load), HFI, or their interaction (Table S7a-b). Juveniles showed lower *Bd*-inhibitory ASV diversity than adults (Table S7a). Sequencing depth was positively associated with Chao1 richness but not with Shannon diversity (Table S7a-b).

Beta diversity of the *Bd*-inhibitory bacterial community showed the same overall patterns as the total skin microbiome. Community similarity decreased with increasing *Bd* load differences and with spatial distance between frogs (Table S8). In contrast, both HFI and age were positively associated with similarity. The interaction between HFI and *Bd* load did not explain variation in beta diversity (95% CI overlapped zero) (Table S8).

4. Discussion

Despite the known influence of habitat disturbance on skin microbiome composition and *Bd* dynamics when studied in isolation, the interaction among the three has been largely overlooked. Our findings suggest that higher human habitat disturbance, here measured as HFI, leads to increased infection prevalence but has a relatively small effect on the skin bacterial communities of *Dendrobates tinctorius*. Instead, *Bd* infection load and geographical

491 distances between populations were strongly associated with microbiome alpha and beta
492 diversity, with patterns that varied across the disturbance gradient. Below, we discuss the
493 potential mechanisms through which HFI may influence *Bd* infection patterns, its interactions
494 with the skin microbiome of *D. tinctorius*, and the implications for disease transmission and
495 ecology.
496
497 *4.1 Patterns of Bd infection in relation to habitat disturbance and spatial aggregation*
498 The probability of *Bd* infection, but not its intensity, increased with HFI, suggesting that human
499 disturbance may influence infection risk. Furthermore, infection probability also increased with
500 proximity to the closest conspecific. This indicates that spatial aggregation affects infection
501 patterns in *D. tinctorius*, potentially through increased transmission rates. Unsurprisingly,
502 patterns of spatial aggregation were mediated by overall population density, with frogs in
503 comparatively denser populations clustering more than those from sparse populations (note
504 that our estimates of nearest-neighbour distance and local density may be slightly biased by
505 increased search effort in locations where frogs had already been found to maximise sample
506 size). These results are consistent with density-dependent *Bd* transmission dynamics (Briggs
507 et al., 2010), and align with previous studies showing higher infection prevalences with
508 increasing contact rates (Malagon et al., 2020) and with species aggregations during the
509 breeding season (Brannelly et al., 2015). However, we found no correlation between HFI and
510 spatial clustering (nearest-neighbour distance and local density) or relative population density,
511 suggesting that HFI affects *Bd* prevalence through density-independent pathways. For
512 example, one possibility is that frogs in more anthropogenically disturbed areas experience
513 chronic stress, which can reduce immune function and overall condition (Hayes et al., 2006;
514 Garcia Neto et al., 2020; Macdonald et al., 2023). Although we could not compare body
515 condition among sites in this study, stress-related immunosuppression has been linked to
516 increased *Bd* susceptibility in other amphibians (Assis et al., 2023). Furthermore, higher
517 human presence and activity in disturbed sites may facilitate the introduction and circulation
518 of *Bd*, increasing its prevalence as found in previous studies (e.g. Bacigalupe et al., 2017;

519 Alvarado-Rybak et al., 2021; de Andrade Serrano et al., 2022). The relationship between
520 human-disturbed habitats and *Bd* prevalence, however, appears to be inconsistent and
521 context-dependent, with multiple studies reporting relatively higher occurrences in pristine
522 areas, where cooler and more humid microclimatic conditions favour the pathogen (Becker &
523 Zamudio, 2011). In our study system, previous work found no significant differences in
524 microhabitat structure or climatic conditions among sites (Mayer et al., 2025). Finally, the
525 disturbed sites sampled in this study likely harboured poorer amphibian species richness,
526 which may have contributed to higher *Bd* risk due to the loss of a potential dilution effect
527 observed in more diverse communities (Searle et al., 2011).
528
529 When comparing the prevalence observed in this study with the first survey reported in the
530 region more than a decade ago (Courtois et al., 2012, 2015), *Bd* prevalence appears to have
531 increased by roughly 10% in Nouragues, whereas in Kaw the estimates are comparable (these
532 being the only two shared sites across studies). In contrast, Courtois et al. (2015) reported no
533 *Bd* detections in the Matoury area, where we observed the highest prevalence in the nearby
534 populations of Petit Matoury and Mont Fortuné (21% and 46% respectively). Moreover,
535 although HFI was not associated with *Bd* load across the full range of infections, the upper
536 10% of infection intensities were disproportionately found in the most disturbed sites (Petit
537 Matoury and Mont Fortuné). Notably, clinical signs of *Bd* (abnormal skin shedding, lethargy,
538 and signs of emaciation) were also recorded in four frogs from these populations, and these
539 individuals were among those with the highest infection loads. Finally, the prevalence estimate
540 for Cacao is based on a much smaller sample size than the other populations and may not be
541 representative, so it should be interpreted with caution.
542
543 Although further research is needed, the observed patterns suggest that *Bd* dynamics vary
544 across populations: Kaw and Nouragues seem to have reached an enzootic state, with
545 infections maintained at relatively constant levels over time, whereas others may be
546 experiencing an epizootic phase, with infection intensifying. Similar within-species variation in

Bd dynamics has been documented in other amphibians, including *Rana muscosa* and *R. sierrae*, where some populations rapidly declined following *Bd* invasion while others persisted long-term with low fungal loads (Briggs et al., 2010). Unfortunately, in this study we cannot disentangle the effects of the timing of *Bd* arrival from those of habitat disturbance, and both factors may have interacted to shape the observed variation in infection dynamics across populations.

4.2 Association between skin microbiome, habitat disturbance and Bd infection

Contrary to our expectations, HFI was not a strong predictor of skin bacterial community composition. We found that alpha diversity was independent from habitat disturbance, with similar values observed across populations (except for Cacao, likely due to its notably smaller sample size). Previous studies reported mixed effects of disturbance, with some finding increases (e.g.Chen et al., 2023), decreases (e.g. Jiménez et al., 2020), or no differences (e.g. Hughey et al., 2017; Bates et al., 2023) depending on species and life stages. In addition, we found only a weak, and unexpected, positive effect of HFI on community similarity. In contrast, spatial distance showed a strong negative correlation with community similarity, suggesting that geographical distance between populations may play a stronger role than habitat disturbance in shaping skin bacterial communities. Local environmental factors such as soil microbiome, soil pH, water chemistry, or vegetation are well-known determinants of host skin microbial structure, composition, and function (Varela et al., 2018; Hernández-Gómez et al., 2020; Bates et al., 2023), and their geographical variation may have therefore resulted in a greater impact on the skin microbiome of *D. tinctorius* than HFI. Similarly, Hughey et al., (2017) found that elevation had a stronger influence than land use on the skin bacterial community of *Eleutherodactylus coqui*.

The major role of the environment in shaping *D. tinctorius* microbiome is further supported by our comparison between wild and captive raised frogs (semi-natural enclosures): despite originating from the same wild populations, the two groups exhibited a markedly distinct skin

bacterial composition. This strong divergence emphasises the importance of complementing lab-based research with field studies, which better capture the environmental complexity necessary for a realistic understanding of the microbiome and disease dynamics. Moreover, these pronounced differences between captive and wild frogs suggest that environmental factors play a much stronger role in shaping skin microbiome structure than underlying genetic differences among populations, even in species with substantial phenotypic differences. Despite the strong environmental influence, wild frogs harboured bacterial communities that were compositionally distinct from the environmental ones.

Among infected frogs, alpha diversity of the overall bacterial community decreased with increasing *Bd* load, with reductions being more pronounced in disturbed habitats. This suggests that frogs with higher infection intensities tend to have poorer or less even microbial communities, especially those from sites with higher HFI, which may already harbour less stable or slightly more stressed microbial communities. Consistent with this, beta diversity increased with *Bd* load, showing that microbial composition became more dissimilar between frogs as differences in infection load intensified. Such patterns align with previous studies reporting that *Bd* infection is associated with substantial changes in skin microbiota structure and composition (Muletz-Wolz et al., 2019; Jani et al., 2021; Bates et al., 2022). Importantly, we found that bacterial dispersion, a measure of health disruption, increased with *Bd* load conditional on HFI. This indicates that frogs exhibited a dysbiotic microbiome state when high infection intensities and habitat disturbance stressors co-occured, consistent with the Anna Karenina Principle, as found in other studies (Jiménez et al., 2020; Neely et al., 2022). Together, these findings suggest that anthropogenic disturbance does not directly restructure the skin microbiome, but instead amplifies *Bd*-driven disruptions. However, because our study is correlational, we cannot determine whether *Bd* infection caused the observed changes or whether frogs with inherently less diverse microbial communities were more susceptible to the pathogen. For example, Buttimer et al. (2025) found that *Brachycephalus rotenbergae* carried higher *Bd* loads after rainfall deficit caused microbiome dysbiosis.

In addition to changes in overall community structure, *Bd* infection load was also associated with a relative abundance increase of putative *Bd*-inhibitory bacteria in more disturbed sites. A similar pattern was reported by Jiménez et al. (2020) for *Lithobates vibicarius*, where a higher representation of *Bd*-inhibitory taxa in disturbed habitats was interpreted as a response to elevated pathogen pressure rather than enhanced protection. Thus, increases in a few inhibitory taxa may reflect compensatory or stress-induced microbial responses to infection.

4.3 Skin microbiome composition and host traits

Overall, the skin bacterial communities of *D. tinctorius* were dominated by Proteobacteria and Bacteroidota, phyla commonly listed as components of the skin microbiome across amphibian species, including tropical taxa and other dendrobatids (Becker et al., 2017; Varela et al., 2018; McGrath-Blaser et al., 2021). Within this community assemblage, however, host characteristics also influenced bacterial diversity and composition.

Juveniles exhibited lower overall alpha diversity, as well as reduced diversity of putative *Bd*-inhibitory taxa compared with adults, suggesting that recently metamorphosed frogs may harbour simpler or more immature microbial communities. Beta diversity analyses further indicated a clear distinction between juveniles and adults, reflecting ontogenic shifts in skin microbiota composition. This aligns with studies showing a strong restructuring from tadpoles to adults (Kueneman et al., 2014; Bataille et al., 2018; Bates et al., 2023). Such reduced skin bacterial diversity in juveniles may lead to higher susceptibility to infection, which could explain the higher *Bd* prevalences and intensities observed in *D. tinctorius* with decreasing size (a proxy for age) (Schlippe-Justicia et al., 2026). However, because our juvenile sample size was too low, we were unable to directly test stage-related differences in infection patterns. Additionally, we found a positive correlation between body condition and overall alpha diversity, as well as with the relative abundance of putative *Bd*-inhibitory taxa among infected frogs. This suggests that individuals in better condition tended to harbour richer and more

631 diverse microbial communities, including a higher proportion of taxa associated with *Bd*
632 inhibition.
633
634 Although we found differences in infection patterns among populations, with prevalences
635 ranging from 7 to 46% and partly related to HFI, it is worth stressing that completely
636 disentangling the effects of general habitat differences (e.g., plant and animal communities,
637 microclimatic conditions, soil composition, frog morphology) from HFI effects on the skin
638 microbiome and disease dynamics is challenging. This is due to the fact that there was virtually
639 no within-site variation in HFI, and that with the number of replicates included in the study we
640 lack the statistical power to fully separate the effects of human-related habitat disturbance
641 from those of potentially confounding effects. In addition, while our results suggest that
642 environmental factors play a stronger role than population origin in shaping the skin
643 microbiome, we did not account for potential genetic differentiation among populations or other
644 host-derived defences. For example, variation in antimicrobial peptides produced by the skin,
645 which are known to play an important role in amphibian immunity (Rollins-Smith, 2009; Mayer
646 et al., 2021), may further contribute to population level-differences in microbiome composition
647 and infection dynamics.
648
649 *4.4 Conclusions*
650 Our findings indicate that anthropogenic habitat disturbance is associated with variation in *Bd*
651 infection patterns in *D. tinctorius*. Disturbance did not directly alter the skin bacterial
652 communities, but it appeared to amplify the negative association between *Bd* load and
653 microbiome alpha diversity. Although causal relationships cannot be inferred from this study,
654 these results suggest that environmental disturbance may interact with pathogen pressure to
655 influence host-microbiome dynamics. In the context of global change, such interacting
656 stressors may increase disease-related vulnerability in amphibian populations, emphasizing
657 the importance of habitat integrity.
658

Acknowledgements.

We are thankful to the staff of CNRS Guyane and the National Forests Office for logistic support, and to Philippe Gaucher and Andrius Pašukonis for important information regarding the locations of the different poison frog populations. We also would like to thank Steve Smith for his advice in the development of the methodology, and to Zuza Zielinska for her assistance in the lab. AI tools were used in a limited capacity to assist with aspects of code refinement and troubleshooting.

Ethics statement

All capture and handling permits were granted by the Direction Générale des Territoires et de la Mer Guyane (DGTM; R03-2022-12-28-00004) after an evaluation by the Regional Scientific Committee (CRSPN). Protocols employed at Nouragues Research Station were also approved by the Reserve 's scientific committee.

Author contributions. Lia Schlippe Justicia: conceptualization, methodology, investigation, formal analysis, visualization, writing – original draft, writing – review and editing. **Susana Ferreira:** formal analysis, visualization, writing – review and editing. **Franz Hoelzl:** conceptualization, methodology, writing – review and editing. **Carolin Dittrich:** investigation, methodology, writing – review and editing. **Martin Mayer:** methodology, investigation, formal analysis, writing – review and editing. **Bibiana Rojas:** conceptualization, funding acquisition, methodology, validation, writing – review and editing, supervision, resources, project administration.

Funding

This study was funded by a grant from the Finnish Research Council (No. 345974) and startup funds from the University of Veterinary Medicine Vienna, both to BR.

Data availability statement

Analyses reported in this article can be reproduced using the data and R scripts provided by Schlippe Justicia et al. (2026).

References

Alvarado-Rybak, M., Lepe-Lopez, M., Peñafiel-Ricaurte, A., Valenzuela-Sánchez, A., Valdivia, C., Mardones, F. O., Bacigalupe, L. D., Puschendorf, R., Cunningham, A. A., & Azat, C. (2021). Bioclimatic and anthropogenic variables shape the occurrence of *Batrachochytrium dendrobatidis* over a large latitudinal gradient. *Scientific Reports*, *11*(1), 17383. https://doi.org/10.1038/s41598-021-96535-w

Arnold, T. W. (2010). Uninformative parameters and model selection using Akaike's Information Criterion. *The Journal of Wildlife Management*, *74*(6), 1175–1178. https://doi.org/10.1111/j.1937-2817.2010.tb01236.x

Assis, V. R., Robert, J., & Titon, S. C. M. (2023). Introduction to the special issue Amphibian immunity: Stress, disease and ecoimmunology. *Philosophical Transactions of the Royal Society B: Biological Sciences*, *378*(1882), 20220117. https://doi.org/10.1098/rstb.2022.0117

Bacigalupe, L. D., Soto-Azat, C., García-Vera, C., Barría-Oyarzo, I., & Rezende, E. L. (2017). Effects of amphibian phylogeny, climate and human impact on the occurrence of the amphibian-killing chytrid fungus. *Global Change Biology*, *23*(9), 3543–3553. https://doi.org/10.1111/gcb.13610

Bataille, A., Lee-Cruz, L., Tripathi, B., & Waldman, B. (2018). Skin bacterial community reorganization following metamorphosis of the fire-bellied toad (*Bombina orientalis*). *Microbial Ecology*, *75*(2), 505–514. https://doi.org/10.1007/s00248-017-1034-7

Bates, K. A., Friesen, J., Loyau, A., Butler, H., Vredenburg, V. T., Laufer, J., Chatzinotas, A., & Schmeller, D. S. (2023). Environmental and anthropogenic factors shape the skin bacterial communities of a semi-arid amphibian species. *Microbial Ecology*, *86*(2), 1393–1404. https://doi.org/10.1007/s00248-022-02130-5

Bates, K. A., Sommer, U., Hopkins, K. P., Shelton, J. M. G., Wierzbicki, C., Sergeant, C., Tapley, B., Michaels, C. J., Schmeller, D. S., Loyau, A., Bosch, J., Viant, M. R., Harrison, X. A., Garner,

T. W. J., & Fisher, M. C. (2022). Microbiome function predicts amphibian chytridiomycosis disease dynamics. *Microbiome*, *10*(1), 44. https://doi.org/10.1186/s40168-021-01215-6

Becker, C. G., Longo, A. V., Haddad, C. F. B., & Zamudio, K. R. (2017). Land cover and forest connectivity alter the interactions among host, pathogen and skin microbiome. *Proceedings of the Royal Society B: Biological Sciences*, *284*(1861), 20170582. https://doi.org/10.1098/rspb.2017.0582

Becker, C. G., & Zamudio, K. R. (2011). Tropical amphibian populations experience higher disease risk in natural habitats. *Proceedings of the National Academy of Sciences*, *108*(24), 9893–9898. https://doi.org/10.1073/pnas.1014497108

Beebee, T. J. C., & Griffiths, R. A. (2005). The amphibian decline crisis: A watershed for conservation biology? *Biological Conservation*, *125*(3), 271–285. https://doi.org/10.1016/j.biocon.2005.04.009

Berger, L., Speare, R., Daszak, P., Green, D. E., Cunningham, A. A., Goggin, C. L., Slocombe, R., Ragan, M. A., Hyatt, A. D., McDonald, K. R., Hines, H. B., Lips, K. R., Marantelli, G., & Parkes, H. (1998). Chytridiomycosis causes amphibian mortality associated with population declines in the rain forests of Australia and Central America. *Proceedings of the National Academy of Sciences*, *95*(15), 9031–9036. https://doi.org/10.1073/pnas.95.15.9031

Brannelly, L. A., Hunter, D. A., Lenger, D., Scheele, B. C., Skerratt, L. F., & Berger, L. (2015). Dynamics of chytridiomycosis during the breeding season in an Australian alpine amphibian. *PLOS ONE*, *10*(12), e0143629. https://doi.org/10.1371/journal.pone.0143629

Bray, J. R., & Curtis, J. T. (1957). An ordination of the upland forest communities of southern Wisconsin. *Ecological Monographs*, *27*(4), 326–349. https://doi.org/10.2307/1942268

Briggs, C. J., Knapp, R. A., & Vredenburg, V. T. (2010). Enzootic and epizootic dynamics of the chytrid fungal pathogen of amphibians. *Proceedings of the National Academy of Sciences*, *107*(21), 9695–9700. https://doi.org/10.1073/pnas.0912886107

Bürkner, P. C. (2017). *brms: Bayesian multilevel models using Stan* (Version 2.19.0) [R package]. Comprehensive R Archive Network. https://CRAN.R-project.org/package=brms

Buttimer, S., Medina, D., Martins, R. A., Da Silva, A. G. M., Neely, W. J., Haddad, C. F. B., DiRenzo, G. V., Catenazzi, A., Bell, R. C., & Becker, C. G. (2025). Experimental drought suppresses

amphibian pathogen yet intensifies transmission and disrupts protective skin microbiome. *Global Change Biology*, *31*(6). https://doi.org/10.1111/gcb.70275

Callahan, B. J., McMurdie, P. J., Rosen, M. J., Han, A. W., Johnson, A. J. A., & Holmes, S. P. (2016). DADA2: High-resolution sample inference from Illumina amplicon data. *Nature Methods*, *13*(7), 581–583. https://doi.org/10.1038/nmeth.3869

Chao, A. (1984). Nonparametric estimation of the number of classes in a population. *Scandinavian Journal of Statistics*, *11*(4), 265–270.

Chen, H., Huang, Y., Pang, G., Cui, Z., Wu, Z., Huang, H., Chen, H., Huang, Y., Pang, G., Cui, Z., Wu, Z., & Huang, H. (2023). Ecological factors and anthropogenic disturbance may restructure the skin microbiota of Maoershan Hynobiids (*Hynobius maoershanensis*). *Diversity*, *15*(8). https://doi.org/10.3390/d15080932

Courtois, E. A., Gaucher, P., Chave, J., & Schmeller, D. S. (2015). Widespread occurrence of *Bd* in French Guiana, South America. *PLOS ONE*, *10*(4), e0125128. https://doi.org/10.1371/journal.pone.0125128

Courtois, E. A., Pineau, K., Villette, B., Schmeller, D. S., & Gaucher, P. (2012). Population estimates of *Dendrobates tinctorius* (Anura: Dendrobatidae) at three sites in French Guiana and first record of chytrid infection. *Phyllomedusa: Journal of Herpetology*, *11*(1), 63–70. https://doi.org/10.11606/issn.2316-9079.v11i1p63-70

Davis, N. M., Proctor, Di. M., Holmes, S. P., Relman, D. A., & Callahan, B. J. (2018). Simple statistical identification and removal of contaminant sequences in marker-gene and metagenomics data. *Microbiome*, *6*(1), 1–14. https://doi.org/10.1186/s40168-018-0605-2

de Andrade Serrano, J., Toledo, L. F., & Sales, L. P. (2022). Human impact modulates chytrid fungus occurrence in amphibians in the Brazilian Atlantic Forest. *Perspectives in Ecology and Conservation*, *20*(3), 256–262. https://doi.org/10.1016/j.pecon.2022.05.002

Ellison, S., Knapp, R. A., Sparagon, W., Swei, A., & Vredenburg, V. T. (2019). Reduced skin bacterial diversity correlates with increased pathogen infection intensity in an endangered amphibian host. *Molecular Ecology*, *28*(1), 127–140. https://doi.org/10.1111/mec.14964

Ferreira, S. C. M., Jarquín-Díaz, V. H., Planillo, A., Ďureje, Ľ., Martincová, I., Kramer-Schadt, S., Forslund-Startceva, S. K., & Heitlinger, E. (2024). Eco-evolutionary dynamics of host–microbiome interactions in a natural population of closely related mouse subspecies and their

hybrids. *Proceedings of the Royal Society B: Biological Sciences*, *291*(2037), 20241970. https://doi.org/10.1098/rspb.2024.1970

Flowers, L., & Grice, E. A. (2020). The skin microbiota: Balancing risk and reward. *Cell Host & Microbe*, *28*(2), 190–200. https://doi.org/10.1016/j.chom.2020.06.017

Garcia Neto, P. G., Nowakowski, A. J., da Silva, A. F. C., Oliveira, O. C. C., Guerra, R. N. M., & de Andrade, G. V. (2020). Leukocyte profiles of two neotropical anuran species affected by anthropogenic habitat alteration. *Animal Conservation*, *23*(5), 524–532. https://doi.org/10.1111/acv.12564

Gomaa, E. Z. (2020). Human gut microbiota/microbiome in health and diseases: A review. *Antonie van Leeuwenhoek*, *113*(12), 2019–2040. https://doi.org/10.1007/s10482-020-01474-7

Haddad, N. M., Brudvig, L. A., Clobert, J., Davies, K. F., Gonzalez, A., Holt, R. D., Lovejoy, T. E., Sexton, J. O., Austin, M. P., Collins, C. D., Cook, W. M., Damschen, E. I., Ewers, R. M., Foster, B. L., Jenkins, C. N., King, A. J., Laurance, W. F., Levey, D. J., Margules, C. R., … Townshend, J. R. (2015). Habitat fragmentation and its lasting impact on Earth's ecosystems. *Science Advances*, *1*(2), e1500052. https://doi.org/10.1126/sciadv.1500052

Harris, R. N., James, T. Y., Lauer, A., Simon, M. A., & Patel, A. (2006). Amphibian pathogen *Batrachochytrium dendrobatidis* is inhibited by the cutaneous bacteria of amphibian species. *EcoHealth*, *3*(1), 53–56. https://doi.org/10.1007/s10393-005-0009-1

Hayes, T. B., Case, P., Chui, S., Chung, D., Haeffele, C., Haston, K., Lee, M., Mai, V. P., Marjuoa, Y., Parker, J., & Tsui, M. (2006). Pesticide mixtures, endocrine disruption, and amphibian declines: Are we underestimating the impact? *Environmental Health Perspectives*, *114*(Suppl 1), 40–50. https://doi.org/10.1289/ehp.8051

Hernández-Gómez, O., Byrne, A. Q., Gunderson, A. R., Jenkinson, T. S., Noss, C. F., Rothstein, A. P., Womack, M. C., & Rosenblum, E. B. (2020). Invasive vegetation affects amphibian skin microbiota and body condition. *PeerJ*, *8*, e8549. https://doi.org/10.7717/peerj.8549

Hoffman, M. D., & Gelman, A. (2014). The No-U-Turn sampler: Adaptively setting path lengths in Hamiltonian Monte Carlo. *Journal of Machine Learning Research, 15*(1), 1593–1623.

Hughey, M. C., Pena, J. A., Reyes, R., Medina, D., Belden, L. K., & Burrowes, P. A. (2017). Skin bacterial microbiome of a generalist Puerto Rican frog varies along elevation and land use gradients. *PeerJ*, *5*, e3688. https://doi.org/10.7717/peerj.3688

Jani, A. J., & Briggs, C. J. (2014). The pathogen *Batrachochytrium dendrobatidis* disturbs the frog skin microbiome during a natural epidemic and experimental infection. *Proceedings of the National Academy of Sciences*, *111*(47), E5049–E5058. https://doi.org/10.1073/pnas.1412752111

Jani, A. J., Bushell, J., Arisdakessian, C. G., Belcaid, M., Boiano, D. M., Brown, C., & Knapp, R. A. (2021). The amphibian microbiome exhibits poor resilience following pathogen-induced disturbance. *The ISME Journal*, *15*(6), 1628–1640. https://doi.org/10.1038/s41396-020-00875-w

Jiménez, R. R., Alvarado, G., Sandoval, J., & Sommer, S. (2020). Habitat disturbance influences the skin microbiome of a rediscovered neotropical-montane frog. *BMC Microbiology*, *20*, 292. https://doi.org/10.1186/s12866-020-01979-1

Kearns, P. J., Fischer, S., Fernández-Beaskoetxea, S., Gabor, C. R., Bosch, J., Bowen, J. L., Tlusty, M. F., & Woodhams, D. C. (2017). Fight fungi with fungi: Antifungal properties of the amphibian mycobiome. *Frontiers in Microbiology*, *8*. https://doi.org/10.3389/fmicb.2017.02494

Kueneman, J. G., Parfrey, L. W., Woodhams, D. C., Archer, H. M., Knight, R., & McKenzie, V. J. (2014). The amphibian skin-associated microbiome across species, space and life history stages. *Molecular Ecology*, *23*(6), 1238–1250. https://doi.org/10.1111/mec.12510

Lahti, L., Shetty, S., Blake, T., & Salojärvi, J. (2020). *microbiome: Tools for microbiome analysis in R* (Version 1.28.0) [R package]. Bioconductor. https://microbiome.github.io/microbiome

Li, J., Bates, K. A., Hoang, K. L., Hector, T. E., Knowles, S. C. L., & King, K. C. (2023). Experimental temperatures shape host microbiome diversity and composition. *Global Change Biology*, *29*(1), 41–56. https://doi.org/10.1111/gcb.16429

Luedtke, J. A., Chanson, J., Neam, K., Hobin, L., Maciel, A. O., Catenazzi, A., Borzée, A., Hamidy, A., Aowphol, A., Jean, A., Sosa-Bartuano, Á., Fong G., A., de Silva, A., Fouquet, A., Angulo, A., Kidov, A. A., Muñoz Saravia, A., Diesmos, A. C., Tominaga, A., … Stuart, S. N. (2023). Ongoing declines for the world's amphibians in the face of emerging threats. *Nature*, *622*(7982), 308–314. https://doi.org/10.1038/s41586-023-06578-4

Macdonald, K. J., Driscoll, D. A., Macdonald, K. J., Hradsky, B., & Doherty, T. S. (2023). Meta-analysis reveals impacts of disturbance on reptile and amphibian body condition. *Global Change Biology*, *29*(17), 4949–4965. https://doi.org/10.1111/gcb.16852

Malagon, D. A., Melara, L. A., Prosper, O. F., Lenhart, S., Carter, E. D., Fordyce, J. A., Peterson, A. C., Miller, D. L., & Gray, M. J. (2020). Host density and habitat structure influence host contact rates and *Batrachochytrium salamandrivorans* transmission. *Scientific Reports*, *10*(1), 5584. https://doi.org/10.1038/s41598-020-62351-x

Mayer, M., Schlippe Justicia, L., & Rojas, B. (2025). Phenotypic divergence across populations does not affect habitat selection in an Amazonian poison frog. *Global Ecology and Conservation*, *57*, e03358. https://doi.org/10.1016/j.gecco.2024.e03358

Mayer, M., Schlippe Justicia, L., Shine, R., & Brown, G. P. (2021). Host defense or parasite cue: Skin secretions mediate interactions between amphibians and their parasites. Ecology Letters, 24(9), 1955–1965. https://doi.org/10.1111/ele.13832

McFall-Ngai, M., Hadfield, M. G., Bosch, T. C. G., Carey, H. V., Domazet-Lošo, T., Douglas, A. E., Dubilier, N., Eberl, G., Fukami, T., Gilbert, S. F., Hentschel, U., King, N., Kjelleberg, S., Knoll, A. H., Kremer, N., Mazmanian, S. K., Metcalf, J. L., Nealson, K., Pierce, N. E., … Wernegreen, J. J. (2013). Animals in a bacterial world, a new imperative for the life sciences. *Proceedings of the National Academy of Sciences*, *110*(9), 3229–3236. https://doi.org/10.1073/pnas.1218525110

McGrath-Blaser, S., Steffen, M., Grafe, T. U., Torres-Sánchez, M., McLeod, D. S., & Muletz-Wolz, C. R. (2021). Early life skin microbial trajectory as a function of vertical and environmental transmission in Bornean foam-nesting frogs. *Animal Microbiome*, *3*(1), 83. https://doi.org/10.1186/s42523-021-00147-8

McLaren, M. R., & Callahan, B. J. (2021). *Silva 138.1 prokaryotic SSU taxonomic training data formatted for DADA2*. https://doi.org/10.5281/zenodo.4587955

McMurdie, P. J., & Holmes, S. (2013). *phyloseq: An R package for reproducible interactive analysis and graphics of microbiome census data* (Version 1.50.0) [R package]. Bioconductor. https://bioconductor.org/packages/phyloseq

Mousavi, S. E., Delgado-Saborit, J. M., Adivi, A., Pauwels, S., & Godderis, L. (2022). Air pollution and endocrine disruptors induce human microbiome imbalances: A systematic review of recent evidence and possible biological mechanisms. *Science of The Total Environment*, *816*, 151654. https://doi.org/10.1016/j.scitotenv.2021.151654

Mu, H., Li, X., Wen, Y., Huang, J., Du, P., Su, W., Miao, S., & Geng, M. (2022). A global record of annual terrestrial Human Footprint dataset from 2000 to 2018. *Scientific Data*, *9*(1), 176. https://doi.org/10.1038/s41597-022-01284-8

Muletz-Wolz, C. R., Fleischer, R. C., & Lips, K. R. (2019). Fungal disease and temperature alter skin microbiome structure in an experimental salamander system. *Molecular Ecology*, *28*(11), 2917–2931. https://doi.org/10.1111/mec.15122

Nakatsuji, T., Cheng, J. Y., & Gallo, R. L. (2021). Mechanisms for control of skin immune function by the microbiome. *Current Opinion in Immunology*, *72*, 324–330. https://doi.org/10.1016/j.coi.2021.09.001

Neely, W. J., Greenspan, S. E., Stahl, L. M., Heraghty, S. D., Marshall, V. M., Atkinson, C. L., & Becker, C. G. (2022). Habitat disturbance linked with host microbiome dispersion and *Bd* dynamics in temperate amphibians. *Microbial Ecology*, *84*(3), 901–910. https://doi.org/10.1007/s00248-021-01897-3

Noonan, B. P., & Gaucher, P. (2006). Refugial isolation and secondary contact in the dyeing poison frog *Dendrobates tinctorius*. *Molecular Ecology*, *15*(14), 4425–4435. https://doi.org/10.1111/j.1365-294X.2006.03074.x

Oksanen, J., Blanchet, F. G., Friendly, M., Kindt, R., Legendre, P., McGlinn, D., Minchin, P. R., O'Hara, R. B., Simpson, G. L., Solymos, P., Stevens, M. H. H., Szoecs, E., & Wagner, H. (2022). *vegan: Community ecology package* (Version 2.6-4) [R package]. Comprehensive R Archive Network. https://CRAN.R-project.org/package=vegan

Pagès, H., Aboyoun, P., Gentleman, R., & DebRoy, S. (2025). *Biostrings: Efficient manipulation of biological strings* (Version 2.78.0) [R package]. Bioconductor. https://bioconductor.org/packages/Biostrings

Pašukonis, A., Serrano-Rojas, S. J., Fischer, M.-T., Loretto, M.-C., Shaykevich, D. A., Rojas, B., Ringler, M., Roland, A. B., Marcillo-Lara, A., Ringler, E., Rodríguez, C., Coloma, L. A., & O'Connell, L. A. (2022). Contrasting parental roles shape sex differences in poison frog space use but not navigational performance. *eLife*, *11*, e80483. https://doi.org/10.7554/eLife.80483

Peig, J., & Green, A. J. (2009). New perspectives for estimating body condition from mass/length data: The scaled mass index as an alternative method. *Oikos*, *118*(12), 1883–1891. https://doi.org/10.1111/j.1600-0706.2009.17643.x

892 Peig, J., & Green, A. J. (2010). The paradigm of body condition: A critical reappraisal of current
893 methods based on mass and length. *Functional Ecology*, *24*(6), 1323–1332.
894 https://doi.org/10.1111/j.1365-2435.2010.01751.x
895 Piovia-Scott, J., Rejmanek, D., Woodhams, D. C., Worth, S. J., Kenny, H., McKenzie, V., Lawler, S.
896 P., & Foley, J. E. (2017). Greater species richness of bacterial skin symbionts better
897 suppresses the amphibian fungal pathogen *Batrachochytrium dendrobatidis*. *Microbial*
898 *Ecology*, *74*(1), 217–226. https://doi.org/10.1007/s00248-016-0916-4
899 Preuss, J. F., Greenspan, S. E., Rossi, E. M., Lucas Gonsales, E. M., Neely, W. J., Valiati, V. H.,
900 Woodhams, D. C., Becker, C. G., & Tozetti, A. M. (2020). Widespread pig farming practice
901 linked to shifts in skin microbiomes and disease in pond-breeding amphibians. *Environmental*
902 *Science & Technology*, *54*(18), 11301–11312. https://doi.org/10.1021/acs.est.0c03219
903 Punzón-Jiménez, P., & Labarta, E. (2021). The impact of the female genital tract microbiome in
904 women health and reproduction: A review. *Journal of Assisted Reproduction and Genetics*,
905 *38*(10), 2519–2541. https://doi.org/10.1007/s10815-021-02247-5
906 QGIS Development Team. (2024). *QGIS geographic information system* (Version 3.30.1) [Software].
907 Open Source Geospatial Foundation. https://qgis.org
908 Quast, C., Pruesse, E., Yilmaz, P., Gerken, J., Schweer, T., Yarza, P., Peplies, J., & Glöckner, F. O.
909 (2013). The SILVA ribosomal RNA gene database project: Improved data processing and
910 web-based tools. *Nucleic Acids Research*, *41*(D1), D590–D596.
911 https://doi.org/10.1093/nar/gks1219
912 R Core Team. (2024). *R: A language and environment for statistical computing* (Version 4.4.2)
913 [Software]. R Foundation for Statistical Computing. https://www.R-project.org
914 Raulo, A., Allen, B. E., Troitsky, T., Husby, A., Firth, J. A., Coulson, T., & Knowles, S. C. L. (2021).
915 Social networks strongly predict the gut microbiota of wild mice. *The ISME Journal*, *15*(9),
916 2601–2613. https://doi.org/10.1038/s41396-021-00949-3
917 Rojas, B., & Endler, J. A. (2013). Sexual dimorphism and intra-populational colour pattern variation in
918 the aposematic frog *Dendrobates tinctorius*. *Evolutionary Ecology*, *27*(4), 739–753.
919 https://doi.org/10.1007/s10682-013-9640-4
920 Rojas, B., & Pašukonis, A. (2019). From habitat use to social behavior: Natural history of a voiceless
921 poison frog, *Dendrobates tinctorius*. *PeerJ*, *7*, e7648. https://doi.org/10.7717/peerj.7648

Rollins-Smith, L. A. (2009). The role of amphibian antimicrobial peptides in protection of amphibians from pathogens linked to global amphibian declines. *Biochimica et Biophysica Acta (BBA) - Biomembranes*, *1788*(8), 1593–1599. https://doi.org/10.1016/j.bbamem.2009.03.008

Rosenberg, E., & Zilber-Rosenberg, I. (2018). The hologenome concept of evolution after 10 years. *Microbiome*, *6*(1), 78. https://doi.org/10.1186/s40168-018-0457-9

Ruthsatz, K., Lyra, M. L., Lambertini, C., Belasen, A. M., Jenkinson, T. S., da Silva Leite, D., Becker, C. G., Haddad, C. F. B., James, T. Y., Zamudio, K. R., Toledo, L. F., & Vences, M. (2020). Skin microbiome correlates with bioclimate and *Batrachochytrium dendrobatidis* infection intensity in Brazil's Atlantic Forest treefrogs. *Scientific Reports*, *10*(1), 22311. https://doi.org/10.1038/s41598-020-79130-3

Sage, R. F. (2020). Global change biology: A primer. *Global Change Biology*, *26*(1), 3–30. https://doi.org/10.1111/gcb.14893

Savage, A. E., & Zamudio, K. R. (2011). MHC genotypes associate with resistance to a frog-killing fungus. *Proceedings of the National Academy of Sciences*, *108*(40), 16705–16710. https://doi.org/10.1073/pnas.1106893108

Scheele, B. C., Pasmans, F., Skerratt, L. F., Berger, L., Martel, A., Beukema, W., Acevedo, A. A., Burrowes, P. A., Carvalho, T., Catenazzi, A., De la Riva, I., Fisher, M. C., Flechas, S. V., Foster, C. N., Frías-Álvarez, P., Garner, T. W. J., Gratwicke, B., Guayasamin, J. M., Hirschfeld, M., … Canessa, S. (2019). Amphibian fungal panzootic causes catastrophic and ongoing loss of biodiversity. *Science*, *363*(6434), 1459–1463. https://doi.org/10.1126/science.aav0379

Schlippe-Justicia, L., Dittrich, C., Nokelainen, O., & Rojas, B. (2026). Defensive colouration is not a reliable indicator of fungal infection in aposematic poison frogs. *Behavioral Ecology*, araf137. https://doi.org/10.1093/beheco/araf137

Schlippe Justicia, L., Ferreira, S., Hoelzl, F., Dittrich, C., Mayer, M., Rojas, B. (2026). Data from: Habitat disturbance interacts with Bd infection to shape the skin bacterial communities of an Amazonian frog. https://doi.org/10.6084/m9.figshare.31771225.

Searle, C. L., Biga, L. M., Spatafora, J. W., & Blaustein, A. R. (2011). A dilution effect in the emerging amphibian pathogen *Batrachochytrium dendrobatidis*. *Proceedings of the National Academy of Sciences*, *108*(39), 16322–16326. https://doi.org/10.1073/pnas.1108490108

952 Shannon, C. E. (1948). A mathematical theory of communication. *The Bell System Technical Journal*,
953 *27*(3), 379–423. https://doi.org/10.1002/j.1538-7305.1948.tb01338.x
954 Siddons, S. R., Bray, M. C., & Searle, C. L. (2020). Higher infection prevalence in amphibians
955 inhabiting human-made compared to natural wetlands. *Journal of Wildlife Diseases*, *56*(4),
956 823–836. https://doi.org/10.7589/2019-09-220
957 Soares, K. O., Da Rocha, T. F., Hale, V. L., Vasconcelos, P. C., do Nascimento, L. J., da Silva, N. M.
958 V., Rodrigues, A. E., & de Oliveira, C. J. B. (2025). Comparing the impact of landscape on the
959 gut microbiome of *Apis mellifera* in Atlantic Forest and Caatinga Biomes. *Scientific Reports*,
960 *15*(1), 5293. https://doi.org/10.1038/s41598-025-85114-y
961 Socolar, J. B., Mills, S. C., Gilroy, J. J., Martínez-Revelo, D. E., Medina-Uribe, C. A., Parra-Sanchez,
962 E., Ramirez-Gutierrez, M., Sand Sæbø, J., Meneses, H. S., Pérez, G., Barlow, J., Ochoa
963 Quintero, J. M., Freckleton, R. P., Haugaasen, T., & Edwards, D. P. (2025). Tropical
964 biodiversity loss from land-use change is severely underestimated by local-scale
965 assessments. *Nature Ecology & Evolution*, *9*(9), 1643–1655. https://doi.org/10.1038/s41559-
966 025-02779-4
967 Stackebrandt, E., & Goebel, B. M. (1994). Taxonomic Note: A place for DNA-DNA reassociation and
968 16S rRNA sequence analysis in the present species definition in bacteriology. *International*
969 *Journal of Systematic and Evolutionary Microbiology*, *44*(4), 846–849.
970 https://doi.org/10.1099/00207713-44-4-846
971 Taugbøl, A., Bærum, K. M., Dervo, B. K., & Fossøy, F. (2021). The first detection of the fungal
972 pathogen *Batrachochytrium dendrobatidis* in Norway with no evidence of population declines
973 for great crested and smooth newts based on modeling on traditional trapping data.
974 *Environmental DNA*, *3*(4), 760–768. https://doi.org/10.1002/edn3.180
975 Varela, B. J., Lesbarrères, D., Ibáñez, R., & Green, D. M. (2018). Environmental and host effects on
976 skin bacterial community composition in Panamanian frogs. *Frontiers in Microbiology*, *9*.
977 https://doi.org/10.3389/fmicb.2018.00298
978 Voyles, J., Young, S., Berger, L., Campbell, C., Voyles, W. F., Dinudom, A., Cook, D., Webb, R.,
979 Alford, R. A., Skerratt, L. F., & Speare, R. (2009). Pathogenesis of chytridiomycosis, a cause
980 of catastrophic amphibian declines. *Science*, *326*(5952), 582–585.
981 https://doi.org/10.1126/science.1176765

Wang, Q., Garrity, G. M., Tiedje, J. M., & Cole, J. R. (2007). Naïve Bayesian classifier for rapid assignment of rRNA sequences into the new bacterial taxonomy. *Applied and Environmental Microbiology*, *73*(16), 5261–5267. https://doi.org/10.1128/AEM.00062-07

Wang, Y., & Xie, Z. (2022). Exploring the role of gut microbiome in male reproduction. *Andrology*, *10*(3), 441–450. https://doi.org/10.1111/andr.13143

Wickham, H. (2024). *ggplot2: Create elegant data visualisations using the grammar of graphics* (Version 4.0.0) [R package]. Comprehensive R Archive Network. https://CRAN.R-project.org/package=ggplot2

Womack, M. C., Steigerwald, E., Blackburn, D. C., Cannatella, D. C., Catenazzi, A., Che, J., Koo, M. S., McGuire, J. A., Ron, S. R., Spencer, C. L., Vredenburg, V. T., & Tarvin, R. D. (2022). State of the Amphibia 2020: A review of five years of amphibian research and existing resources. *Ichthyology & Herpetology*, *110*(4), 638–661. https://doi.org/10.1643/h2022005

Woodhams, D. C., Ardipradja, K., Alford, R. A., Marantelli, G., Reinert, L. K., & Rollins-Smith, L. A. (2007). Resistance to chytridiomycosis varies among amphibian species and is correlated with skin peptide defenses. *Animal Conservation*, *10*(4), 409–417. https://doi.org/10.1111/j.1469-1795.2007.00130.x

Woodhams, D. C., Brandt, H., Baumgartner, S., Kielgast, J., Küpfer, E., Tobler, U., Davis, L. R., Schmidt, B. R., Bel, C., Hodel, S., Knight, R., & McKenzie, V. (2014). Interacting symbionts and immunity in the amphibian skin mucosome predict disease risk and probiotic effectiveness. *PLOS ONE*, *9*(4), e96375. https://doi.org/10.1371/journal.pone.0096375

Woodhams, D. C., Alford, R. A., Antwis, R. E., Archer, H., Becker, M. H., Belden, L. K., Bell, S. C., Bletz, M., Daskin, J. H., Davis, L. R., Flechas, S. V., Lauer, A., Gonzalez, A., Harris, R. N., Holden, W. M., Hughey, M. C., Ibáñez, R., Knight, R., Kueneman, J., … McKenzie, V. (2015). Antifungal isolates database of amphibian skin-associated bacteria and function against emerging fungal pathogens. *Ecology*, *96*(2), 595–595. https://doi.org/10.1890/14-1837.1

Woodhams, D. C., LaBumbard, B. C., Barnhart, K. L., Becker, M. H., Bletz, M. C., Escobar, L. A., Flechas, S. V., Forman, M. E., Iannetta, A. A., Joyce, M. D., Rabemananjara, F., Gratwicke, B., Vences, M., & Minbiole, K. P. C. (2018). Prodigiosin, violacein, and volatile organic compounds produced by widespread cutaneous bacteria of amphibians can inhibit two

1011 Batrachochytrium fungal pathogens. *Microbial Ecology*, *75*(4), 1049–1062.
1012 https://doi.org/10.1007/s00248-017-1095-7
1013 Yu, Y., Lee, C., Kim, J., & Hwang, S. (2005). Group-specific primer and probe sets to detect
1014 methanogenic communities using quantitative real-time polymerase chain reaction.
1015 *Biotechnology and Bioengineering*, *89*(6), 670–679. https://doi.org/10.1002/bit.20347
1016 Zaneveld, J. R., McMinds, R., & Vega Thurber, R. (2017). Stress and stability: Applying the Anna
1017 Karenina principle to animal microbiomes. *Nature Microbiology*, *2*(9), 17121.
1018 https://doi.org/10.1038/nmicrobiol.2017.121
1019

SUPPLEMENTARY MATERIAL

Habitat disturbance interacts with Bd infection to shape the skin bacterial communities of an Amazonian frog

Table S1. Summary of models examining (a) *Bd* infection probability and (b) *Bd* infection load in *Dendrobates tinctorius*. For each model, we report parameter estimates, standard errors (SE), and the lower (LCI) and upper (UCI) bounds of the 95% confidence intervals (CI). Effects are considered informative when the 95% CI does not overlap zero and are highlighted in bold.

Predictor	Estimate ± SE	95% CI (LCI - UCI)
(a) Probability of Bd infection		
Intercept	**-1.25 ± 0.24**	**-1.75 – -0.79**
HFI	**0.47 ± 0.23**	**0.02 – 0.95**
Sex (Juvenile)	-0.33 ± 3.37	-10.4 – 5.19
Sex (Male)	-0.53 ± 0.39	-1.33 – 0.21
NND	**-0.57 ± 0.34**	**-1.32 – -0.003**
Local density	-0.02 ± 0.21	-0.46 – 0.37
Elevation	0.20 ± 0.24	-0.26 – 0.68
SVL	-0.16 ± 0.34	-0.84 – 0.51
Sex (Juvenile) x SVL	0.39 ± 1.34	-3.29 – 2.78
Sex (Male) x SVL	0.06 ± 0.62	-1.24 – 1.22
(b) Bd load		
Intercept	**2.24 ± 0.53**	**1.18 – 3.30**
HFI	-0.77 ± 0.74	-2.26 – 0.72
Sex (Juvenile)	12.53 ± 23.4	-34.8 – 59.9
Sex (Male)	0.31 ± 0.92	-1.56 – 2.18
NND	0.14 ± 0.56	-1.00 – 1.27
Local density	-0.25 ± 0.58	-1.43 – 0.93
Elevation	-0.75 ± 0.58	-1.92 – 0.42
SVL	**-1.79 ± 0.82**	**-3.45 – -0.13**
Sex (Juvenile) x SVL	5.65 ± 8.63	-11.80 – 23.09
Sex (Male) x SVL	1.18 ± 1.46	-1.77 – 4.13

Table S2. Model summaries for (*a*) nearest-neighbour distance, and (*b*) local density in *Dendrobates tinctorius*. For each model, we report parameter estimates, standard errors (SE), and the lower (LCI) and upper (UCI) bounds of the 95% confidence intervals (CI). Effects are considered informative when 95% CI does not overlap zero and are highlighted in bold.

Predictor	**Estimate ± SE**	**95% CI (LCI - UCI)**
(a) Nearest-neighbour distance		
HFI	-0.005 ± 0.08	-0.17 – 0.16
Population density	**-0.39 ± 0.08**	**-0.56 – -0.23**
Sex (male)	**-0.47 ± 0.17**	**-0.81 – -0.12**
Sex (juvenile)	-0.53 ± 0.35	-1.21 – 0.16
(b) Local density		
HFI	0.03 ± 0.08	-0.13 – 0.19
Population density	**0.22 ± 0.09**	**0.04 – 0.39**
Sex (male)	0.31 ± 0.17	-0.04 – 0.65
Sex (juvenile)	**0.70 ± 0.32**	**0.08 – 1.33**

Table S3. Model estimates ± standard errors (SE), and 95% confidence intervals (CI) for the alpha diversity (Chao1 and Shannon) analysis of the **overall skin bacterial community** of *D. tinctorius*. Results are shown for models with explanatory variable *Bd* representing (a) *Bd* infection status and (b) *Bd* load. Informative parameters are shown in bold (95% CI do not overlap zero).

Predictor	**Chao1**		**Shannon**	
	Estimate ± SE	**95% CI**	**Estimate ± SE**	**95% CI**
(a) Bd infection status				
Intercept	**-2021.21 ± 515**	**-3036.2 – -1006.2**	**4.7 ± 2.35**	**0.07 – 9.34**
Bd infected (yes)	-35.65 ± 35.1	-104.82 – 33.51	-0.25 ± 0.16	-0.57 – 0.06
HFI	3.39 ± 16.1	-28.38 – 35.18	0.03 ± 0.07	-0.11 – 0.18
Sex (Juvenile)	**-201.47 ± 59.2**	**-318.1 – -84.84**	**-0.69 ± 0.27**	**-1.22 – -0.16**
Sex (Male)	-28.73 ± 29.1	-85.98 – 28.52	-0.08 ± 0.13	-0.34 – 0.18
SMI	**29.08 ± 13.8**	**1.79 – 56.37**	**0.13 ± 0.06**	**0.01 – 0.26**
Depth	**261.57 ± 51.2**	**160.6 – 362.55**	0.02 ± 0.23	-0.44 – 0.48
Infected x HFI	-7.15 ± 32.4	-70.95 – 56.65	-0.01± 0.15	-0.30 – 0.29
(b) Bd load				
Intercept	**-3074.03 ± 1062**	**-5218.51 – -929.5**	-1.02 ± 4.26	-9.63 – 7.59
***Bd* load**	**-74.89 ± 30.3**	**-136 – -13.78**	**-0.42 ± 0.12**	**-0.67 – -0.18**
HFI	5.63 ± 28.7	-52.27 – 63.53	**0.09** ± 0.12	-0.14 – 0.32
Sex (Juvenile)	-249.89 ± 146	-544.68 – 44.89	**-1.23 ± 0.59**	**-2.41 – -0.05**
Sex (Male)	-27.43 ± 65.9	-160.48 – 105.62	-0.05 ± 0.26	-0.58 – 0.48
SMI	-3.28 ± 29.7	-63.29 – 56.73	0.01 ± 0.12	-0.23 – 0.25
Depth	**362.77 ± 106**	**149.03 – 576.5**	0.57 ± 0.43	-0.29 – 1.43
***Bd* load x HFI**	-39.87 ± 29.7	-99.91 – 20.17	**-0.29 ± 0.12**	**-0.53 – -0.05**

Table S4. Shown are the Bayesian multi-membership regression models examining the associations between host and ecological predictors and the skin microbiome similarity (Bray-Curtis distances). Models were fitted using all sequenced ASVs for all wild frogs (n = 230) and for adults only (n = 216). Shown are the posterior mean estimates of the distribution for each predictor and the corresponding lower (LCI) and upper (UCI) bounds of the 95% credible intervals (CI). All models showed good convergence (R-hat < 1.01). Informative parameters are shown in bold (95% CI do not overlap zero).

Predictor	**Estimate**	**LCI**	**UCI**	**Estimate**	**LCI**	**UCI**
	All wild frogs			Adults only wild frogs		
Intercept	**0.22**	**0.20**	**0.23**	**0.24**	**0.23**	**0.25**
Spatial distance	**-0.03**	**-0.03**	**-0.02**	**-0.03**	**-0.03**	**-0.02**
Age (same)	**0.02**	**0.02**	**0.03**	-	-	-
Sex (same)	-	-	-	-0.00	-0.002	0.002
HFI diff.	**0.01**	**0.00**	**0.01**	**0.01**	**0.005**	**0.01**
***Bd* load diff.**	**-0.03**	**-0.04**	**-0.02**	**-0.03**	**-0.04**	**-0.02**
HFI x *Bd* load	-0.003	-0.01	0.01	-0.002	-0.01	0.01

Table S5. Linear model results for the effect of *Bd* load and Human Footprint Index (HFI) on the **skin bacterial community dispersion** (distance to centroid, Bray-Curtis) of *D. tinctorius*. Shown are the estimates ± standard errors (SE), and the corresponding lower (LCI) and upper (UCI) bounds of the 95% confidence intervals (CI). Informative parameters are highlighted in bold (95% CI do not overlap zero).

Predictor	**Estimate ± SE**	**95% CI (LCI - UCI)**
Intercept	0.55 ± 0.004	0.54 – 0.56
Bd load	0.0004 ± 0.004	-0.01 – 0.01
HFI	0.003 ± 0.004	-0.005 – 0.01
***Bd* load x HFI**	**0.01 ± 0.004**	**0.004 – 0.15**

Table S6. Beta-binomial model results for the effects on the **relative abundance of putative *Bd*-inhibitory bacterial taxa** on the skin of *D. tinctorius* including (a) *Bd* infection status and (b) *Bd* load. Shown are the estimates ± standard errors (SE), and the corresponding lower (LCI) and upper (UCI) bounds of the 95% confidence intervals (CI). Informative parameters are highlighted in bold (95% CI do not overlap zero).

Predictor	**Estimate ± SE**	**95% CI**
(a) Bd infection status		
Intercept	**-2.16 ± 0.06**	**-2.28 – -2.03**
Bd infected (yes)	0.06 ± 0.11	-0.15 – 0.27
HFI	-0.06 ± 0.05	-0.16 – 0.04
Sex (Juvenile)	0.01 ± 0.18	-0.34 – 0.37
Sex (Male)	0.05 ± 0.09	-0.12 – 0.22
SMI	-0.02 ± 0.04	-0.11 – 0.06
Infected x HFI	0.12 ± 0.10	-0.07 – 0.31
(a) Bd load		
Intercept	**-2.08 ± 0.13**	**-2.34 – -1.81**
Bd load	0.18 ± 0.10	-0.01 – 0.37
HFI	0.03 ± 0.10	-0.16 – 0.22
Sex (Juvenile)	-0.69 ± 0.54	-1.74 – 0.36
Sex (Male)	0.13 ± 0.21	-0.29 – 0.54
SMI	**0.17 ± 0.09**	**0.002 – 0.35**
***Bd* load x HFI**	**0.29 ± 0.10**	**0.08 – 0.49**

Table S7. Model estimates ± standard errors (SE), and 95% confidence intervals (CI) for the alpha diversity (Chao1 and Shannon) analysis of the **putative *Bd*-inhibitory bacteria** of *D. tinctorius*. Results are shown for models with explanatory variable *Bd* representing (a) *Bd* infection status and (b) *Bd* load. Informative parameters are shown in bold (95% confidence intervals do not overlap zero).

(b) *Bd* load. Informative parameters are shown in bold (95% confidence intervals do not overlap zero).

Predictor	**Chao1**		**Shannon**	
	Estimate ± SE	**95% CI**	**Estimate ± SE**	**95% CI**
(a) Bd infection status				
Intercept	**54.8 ± 1.80**	**51.2 – 58.3**	**2.89 ± 0.07**	**2.75 – 3.04**
Bd infected (yes)	0.59 ± 3.16	-5.63 – 6.81	0.08 ± 0.13	-0.17 – 0.33
HFI	-1.79 ± 1.45	-4.65 – 1.06	-0.01 ± 0.06	-0.12 – 0.11
Sex (Juvenile)	**-18.0 ± 5.32**	**-28.5 – -7.49**	**-0.71 ± 0.21**	**-1.13 – -0.29**
Sex (Male)	-0.20 ± 2.61	-5.35 – 4.94	-0.03 ± 0.10	-0.24 – 0.18
SMI	0.45 ± 1.24	-2.01 – 2.90	-0.01 ± 0.05	-0.11 – 0.09
Depth	**6.73 ± 1.25**	**4.28 – 9.19**	0.09 ± 0.05	-0.01 – 0.19
Bd infected x HFI	-1.67 ± 2.91	-7.40 – 4.07	-0.02 ± 0.12	-0.25 – 0.21
(b) Bd load				
Intercept	**54.5 ± 3.06**	**48.3 – 60.7**	**2.91 ± 0.12**	**2.67 – 3.15**
Bd load	-1.54 ± 2.60	-8.31 – 1.63	-0.16 ± 0.10	-0.36 – 0.05
HFI	-3.34 ± 2.46	-6.78 – 3.71	-0.01 ± 0.09	-0.20 – 0.18
Sex (Juvenile)	-25.2 ± 12.5	-50.5 – 0.14	-0.88 ± 0.49	-1.87 – 0.10
Sex (Male)	-1.66 ± 5.65	-13.1 – 9.76	0.19 ± 0.22	-0.26 – 0.63
SMI	2.78 ± 2.55	-2.38 – 7.93	-0.01 ± 0.10	-0.21 – 0.19
Depth	**8.47 ± 2.59**	**3.23 – 13.7**	0.13 ± 0.10	-0.07 – 0.33
Bd load x HFI	4.06 ± 2.55	-1.10 – 9.21	-0.03 ± 0.10	-0.23 – 0.17

Table S8. Shown is the Bayesian multi-membership regression model examining the associations between host and ecological predictors and the similarity (1 - Bray-Curtis distances) of the community of putative *Bd*-inhibitory bacteria. Shown are the posterior mean estimates of the distribution for each predictor and the corresponding lower (LCI) and upper (UCI) bounds of the 95% credible intervals (CI). All models showed good convergence (R-hat < 1.01). Informative parameters are shown in bold (95% CI do not overlap zero).

Predictor	Estimate	LCI	UCI
Intercept	**0.14**	**0.12**	**0.15**
Spatial distance	**-0.04**	**-0.04**	**-0.03**
Age (same)	**0.02**	**0.01**	**0.03**
HFI diff.	**0.02**	**0.01**	**0.02**
***Bd* load diff.**	**-0.02**	**-0.03**	**-0.01**
HFI x *Bd* load	0.00	-0.01	0.01

Fig S1. For the analysis of the putative *Bd*-inhibitory bacteria in the skin of *D.tinctorius*, (a) comparison of Shannon diversity in uninfected vs *Bd*-infected frogs, showing no clear difference between groups; (b) effect of the interaction between *Bd* load and Human Footprint Index (HFI) on the relative abundance. HFI was treated as a continuous variable in the models but shown grouped into three categories for visualization only (Low: HFI < 5; Medium: 5 – 19; High: > 19).